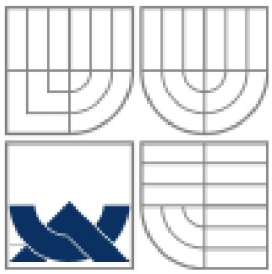

VYSOKÉ UČENÍ TECHNICKÉ V BRNĚ

BRNO UNIVERSITY OF TECHNOLOGY

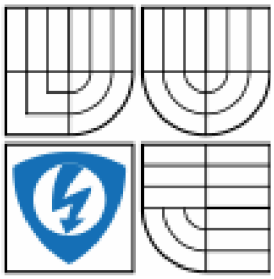

FAKULTA ELEKTROTECHNIKY A KOMUNIKAČNÍCH TECHNOLOGIÍ
ÚSTAV AUTOMATIZACE A MĚŘICÍ TECHNIKY

FACULTY OF ELECTRICAL ENGINEERING AND COMMUNICATION
DEPARTMENT OF CONTROL AND INSTRUMENTATION

MODELING OF THE VERTICAL FLIGHT PROFILE

MODELOVÁNÍ VERTIKÁLNÍHO PROFILU LETU

DIPLOMOVÁ PRÁCE
MASTER'S THESIS

AUTOR PRÁCE
AUTHOR

Bc. JOSEF VALÍČEK

VEDOUCÍ PRÁCE
SUPERVISOR

Ing. PAVEL KUČERA, Ph.D.

BRNO 2011

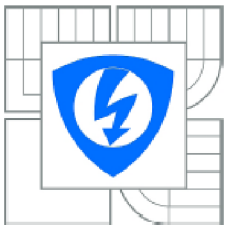

VYSOKÉ UČENÍ
TECHNICKÉ V BRNĚ

Fakulta elektrotechniky
a komunikačních technologií

Ústav automatizace a měřicí techniky

Diplomová práce

magisterský navazující studijní obor
Kybernetika, automatizace a měření

Student:	Bc. Josef Valíček	***ID:***	72778
Ročník:	2	***Akademický rok:***	2010/2011

NÁZEV TÉMATU:

Modeling of the Vertical Flight Profile

POKYNY PRO VYPRACOVÁNÍ:

Acquaint yourself with the General Equations of Motion and set up the aircraft model.
Modify this model by a time-varying mass parameter, set up model parameters according to a real aircraft and simulate it for a continuous cruise climb.
Attempt to make a linearization of this model by a suitable method and try to design state regulator with the aim to optimize vertical flight profile of the aircraft.

DOPORUČENÁ LITERATURA:

RAUW, M.O.: "FDC 1.4 - A Simulink Toolbox for Flight Dynamics and Control Analysis". Zeist, The Netherlands, 1977 (draft version 7: Haarlem, The Netherlands, 2001. ISBN 90-807177-1-1.
ROSKAM, J.: "Airplane Flight Dynamics and Automatic Flight Controls", Roskam Aviation and Engineering corporation, 1994. ISBN 1-884885-18-7.

Termín zadání:	7.2.2011	***Termín odevzdání:***	23.5.2011

Vedoucí práce: Ing. Pavel Kučera, Ph.D.

prof. Ing. Pavel Jura, CSc.
Předseda oborové rady

UPOZORNĚNÍ:

Abstract

The master thesis deals with modeling of aircraft and simulation of types of flight. The long range business jet plane Gulfstream G550 was selected for modeling of the vertical flight profile.

In the first part of the thesis, the aircraft equations of motion are introduced in detail. Further, it is described a numerical model of an aircraft compiled on basics of the equations of motion. This model is used for modeling and vertical profiles of flight simulation. In the next part, the thesis is focused on matching the parameters for the aircraft model according to the Gulfstream G550 and on the theoretical framework of simulation the Continuous Climbing Cruise. The last point of the thesis deal with a research of the fuel optimal Continuous Climbing Cruise. In the conclusion there are discussed some results which has been achieved and the future possibility to follow-up in this work.

Keywords

Vertical flight profile, Equations of motion, Aircraft model, Continuous climbing cruise

Abstrakt

Diplomová práce se zabývá modelováním letadla a simulací různých typů letu. Pro modelování letu bylo podle zadání vybráno proudové letadlo s dlouhým doletem – Gulfstream G550.

V první části práce jsou podrobně popsány pohybové rovnice letadla. Dále je vysvětlen numerický model letadla, sestavený na základě pohybových rovnic. Pochopení modelu letadla je nezbytné pro modelování a simulaci vertikálních profilů letu. Práce se zaměřuje na nastavení parametrů modelu letadla podle reálného letadla Gulfstream G550 a modelování vertikálního profilu letu v letové fázi CRUISE. Posledním bodem práce je průzkum optimálního letu letadla vzhledem ke spotřebě paliva. V závěru jsou diskutovány dosažené výsledky a je nastíněn směr případného pokračování práce.

Klíčová slova

Vertikální profil letu, Pohybové rovnice, Model letadla, Průběžné stoupání letadla

Bibliografická citace:

VALÍČEK, J. *Modeling of the Vertical Flight Profile*. Brno: Vysoké učení technické v Brně, Fakulta elektrotechniky a komunikačních technologií, 2011. 77s. Vedoucí diplomové práce Ing. Pavel Kučera, Ph.D.

Prohlášení

„Prohlašuji, že svou diplomovou práci na téma Modeling of the Vertical Flight Profile jsem vypracoval samostatně pod vedením vedoucího diplomové práce a s použitím odborné literatury a dalších informačních zdrojů, které jsou všechny citovány v práci a uvedeny v seznamu literatury na konci práce.
Jako autor uvedené diplomové práce dále prohlašuji, že v souvislosti s vytvořením této diplomové práce jsem neporušil autorská práva třetích osob, zejména jsem nezasáhl nedovoleným způsobem do cizích autorských práv osobnostních a jsem si plně vědom následků porušení ustanovení § 11 a následujících autorského zákona č. 121/2000 Sb., včetně možných trestněprávních důsledků vyplývajících z ustanovení části druhé, hlavy VI. díl 4 Trestního zákoníku č. 40/2009 Sb.

V Brně dne: **23. května 2011** ……
podpis autora

Poděkování

Děkuji vedoucím diplomové práce Ing. Pavlovi Kučerovi, Ph.D. a Ing. Petru Krupanskému, Ph.D. za účinnou metodickou, pedagogickou a odbornou pomoc a další cenné rady při zpracování mé diplomové práce.

V Brně dne: **23. května 2011** ……
podpis autora

CONTENTS

LIST OF ACRONYMS AND SYMBOLS

Symbols

a	[ms^{-1}]	speed of sound
AR	[–]	aspect ratio
b	[m]	wing-span
c	[m]	mean aerodynamic chord
C_D	[–]	drag coefficient
C_{D0}	[–]	nominal drag coefficient
C_L	[–]	lift coefficient
C_{L0}	[–]	nominal lift coefficient
$C_{L\alpha}$	[–]	lift coefficient of angle of attack
C_m	[–]	pitching moment coefficient
C_{mq}	[–]	pitching moment coefficient of angular rate pitch
$C_{m\alpha}$	[–]	pitching moment coefficient of angle of attack
$C_{m\delta e}$	[–]	pitching moment coefficient of elevator
C_T	[–]	thrust coefficient
D	[N]	total aerodynamic drag
e	[–]	Oswald efficiency number
F_B		body-fixed reference frame
F_E		Earth-fixed reference frame
F_V		vehicle-carried vertical reference frame
F_W		flight-path reference frame
F_x	[N]	total external force along X_B-axis, see Figure 2.1
Fx_a	[N]	aerodynamic force along X_B-axis
F_{Xgr}	[N]	gravity force along X_B-axis
F_{Xp}	[N]	propulsive force along X_B-axis
F_y	[N]	total external force along Y_B-axis, see Figure 2.1
F_{Ya}	[N]	aerodynamic force along Y_B-axis
F_{Ygr}	[N]	gravity force along Y_B-axis
F_{Yp}	[N]	propulsive force along Y_B-axis
F_z	[N]	total external force along Z_B-axis, see Figure 2.1
F_{Za}	[N]	aerodynamic force along Z_B-axis
F_{Zgr}	[N]	gravity force along Z_B-axis
F_{Zp}	[N]	propulsive force along Z_B-axis
g	[ms^{-2}]	acceleration of gravity
H	[FL]	altitude
I_x	[kgm^2]	moment of inertia along X_B-axis
I_y	[kgm^2]	moment of inertia along Y_B-axis
I_z	[kgm^2]	moment of inertia along Z_B-axis
J_{xy}	[kgm^2]	product of inertia in X_BY_B-plane

J_{xz}	[kgm^2]	product of inertia in X_BZ_B-plane
J_{yz}	[kgm^2]	product of inertia in Y_BZ_B-plane
L	[Nm]	total rolling moment, see Figure 2.1
L	[N]	total aerodynamic lift
L_a	[Nm]	aerodynamic rolling moment
L_p	[Nm]	propulsion rolling moment
L/D	[–]	Lift to Drag ratio
m	[kg]	mass of the aircraft
M	[–]	Mach number
M	[Nm]	total pitching moment, see Figure 2.1
M_a	[Nm]	aerodynamic pitching moment
M_p	[Nm]	propulsion pitching moment
N	[Nm]	total yawing moment, see Figure 2.1
N_a	[Nm]	aerodynamic yawing moment
N_p	[Nm]	propulsion yawing moment
p	[rad s^{-1}]	angular rate of roll, see Figure 2.1
P_l , P_m, P_n, P_{pp}, P_{pq}, P_{pr}, P_{qq}, P_{qr}, P_{rr}		inertia coefficients for p-equation,
p_s	[Nm^{-2}]	ambient or free-stream pressure
q	[rad s^{-1}]	angular rate of pitch, see Figure 2.1
q_{dyn}	[Nm^{-2}]	dynamic pressure
Q_l , Q_m, Q_n, Q_{pp}, Q_{pq}, Q_{pr}, Q_{qq}, Q_{qr}, Q_{rr}		inertia coefficients for q-equation,
r	[rad s^{-1}]	angular rate or yaw, see Figure 2.1
R_l , R_m, R_n, R_{pp}, R_{pq}, R_{pr}, R_{qq}, R_{qr}, R_{rr}		inertia coefficients for r-equation,
S	[m^2]	wing area
t	[s]	time
T	[K]	ambient or free-stream temperature
T	[N]	Thrust force
u	[ms^{-1}]	velocity component along X_B-axis
u_w	[ms^{-1}]	wind velocity component along X_B-axis
$\dot{u}_w$	[ms^{-2}]	wind acceleration component along X_B-axis

v	[ms^{-1}]	velocity component along Y_B-axis
v_w	[ms^{-1}]	wind velocity component along Y_B-axis
$\dot{v}_w$	[ms^{-2}]	wind acceleration component along Y_B-axis
V	[ms^{-1}]	true airspeed, see Figure 2.1
w	[ms^{-1}]	velocity component along Z_B-axis
w_w	[ms^{-1}]	wind velocity component along Z_B-axis
$\dot{w}_w$	[ms^{-2}]	wind acceleration component along Z_B-axis
W	[N]	aircraft weight
x_e	[m]	X-coordinate in Earth-fixed reference frame F_E
y_e	[m]	Y-coordinate in Earth-fixed reference frame F_E
z_e	[m]	Z-coordinate in Earth-fixed reference frame F_E
α	[°]	angle of attack, see Figure 2.1
β	[°]	sideslip angle, see Figure 2.1
γ	[°]	flight-path angle
Γ		engine setting
δ_a	[°]	deflection of ailerons
δ_e	[°]	deflection of elevator
δ_f	[°]	deflection of flaps
δ_r	[°]	deflection of rudder
Δ		difference
θ	[°]	pitch angle
μ	[$kgm^{-1}s^{-1}$]	dynamic viscosity
ρ	[kgm^{-3}]	air density
φ	[°]	roll angle
ψ	[°]	yaw angle

Vectors

$\mathbf{C}_{aero}$	vector with non-dimensional aerodynamic force and moment coefficients
Dtheta	vector with reference pitch angle
F	resulting force vector acting on rigid body; $F = [F_x\ F_y\ F_z]^T$
GM	geometrical data vector
h	resulting angular momentum of rigid body about c.g.; $h = [h_x\ h_y\ h_z]^T$
I	inertia vector
i	unit vector along x-axis
j	unit vector along y-axis
k	unit vector along z-axis
M	resulting moment vector about c.g. of rigid body; $M = [L\ M\ N]^T$
r	position vector
u...	input vectors
v	disturbance vector
V	true airspeed vector

x	state vector
y...	output vectors
Ω	rotational velocity vector

Matrices

A	system matrix of linear state-space system
B	input matrix of linear state-space system
C	output matrix of linear state-space system due to **x**
D	output matrix of linear state-space system due to **u**

Functions

f(t)	general vector-equation for the time-derivatives of the state variables
g(t)	general vector-equation for the output variables

Indices and subscripts

0	initial value
a	ailerons
ad	airdata
aero	aerodynamic forces and moments or force and moment coefficients
atm	atmosphere data
dl	dimensionless
e	elevator
e	relative to Earth axes (used for velocity components – u_e, v_e , w_e)
en	engine
f	flaps
grav	gravity force components
prop	engine forces and moments (‘propulsive’)
r	rudder
tot	total components
w	wind velocity and wind velocity components along body axes
wind	force components due to non-steady atmosphere
w_e	wind velocity components along Earth axes

In the thesis, the units of all physical variables are considered in the metric system. Only the altitude (H) is expressed in the FL, which is a standard nominal altitude, in hundreds of feet. This unit is commonly used in the aviation.

Abbreviations

ATC	Air Traffic Control
ATM	Air Traffic Management
A/P	Auto Pilot
A/THR	Auto Thrust
CCC	Continuous Climbing Cruise
c.g.	center of gravity
CI	Cost Index
CRZ FL	Cruise Flight Level
FD	Flight Director
FF	Fuel Flow
FL	Flight Level – is a standard nominal altitude, in hundreds of feet
FG	Flight Guidance functions
FM	Flight Management functions
FMS	Flight Management System
FMGS	Flight Management & Guidance System
ICAO	International Civil Aviation Organization
LQ	Linear Quadratic
MC	Mach number Controller
MDCU	Multifunction Control Display Unit
ND	Navigation Display
ODE	Ordinary Differential Equation
OPTIM	MATLAB Optimization Toolbox
PAC	Pitch Angle Controller
PFD	Primary Flight Display
PI	Proportional and Integrating regulator
PID	Proportional and Integrating and Derivative regulator
RC	Rate of Climb
SES	Single European Sky
SESAR	Single European Sky ATM Research Program
SPD LIMIT	Speed Limit
TOC	Top of Climb
TOD	Top of Descent
X-PLANE	Flight Simulator
ZFCG	Zero Fuel Center of Gravity

LIST OF FIGURES

LIST OF TABLE

1. INTRODUCTION

1.1 BACKGROUND

The SESAR (Single European Sky ATM Research) has been launched by the European Commission in 2004 with the aim to meet future air traffic capacity and safety needs. This ambitious project represents technological dimension of the Single European Sky (SES) initiative. Nowadays there are verified current planning methods of the ATM (Air Traffic Management), however also new and more efficient planning methods are researched. The aim of this thesis is to contribute to modern research in this area. The thesis has been written with the cooperation of the Honeywell Company.

The example of the complete vertical flight profile is defined by the Figure 1.1. There are five main flight phases: Take-off, Climb, Cruise, Descent and Approach. To define fuel optimal vertical flight profile is not trivial, because it depends on the many factors, for example the aircraft types, the aircraft gross weight, ambient environmental conditions, the flight plan, the Air Traffic Control constraints, etc. The fuel optimal vertical flight profile used is approximated by steps through discrete standard flight levels, so the fuel consumption and emissions can be reduced by implementation of continuous vertical flight profile. Generally, the thesis is focused on determining the fuel optimal vertical flight profile in the cruise phase, where the level flight is mostly used. All the simulation and proposal are derived according to the cruise phase.

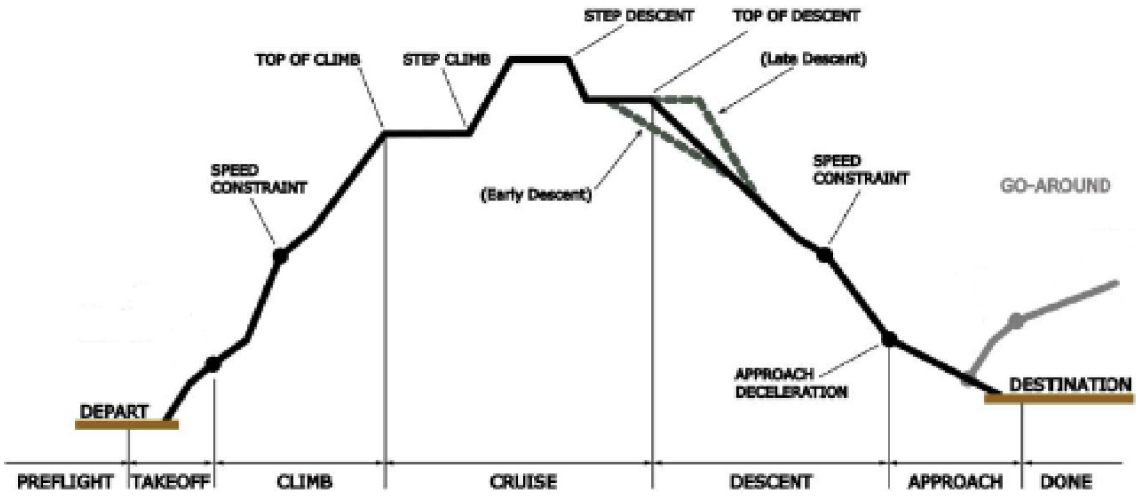

Figure 1.1: Example of the vertical flight profile [5]

The theoretical background of the cruise phase is shown in chapter 5. The cruise phase is defined by the vertical flight profile from the top of climb (TOC) to the top of descent (TOD). The cruise phase is usually the longest phase. An aircraft is less restricted by the ATC, than in the other phases. There are three defined types of an aircraft flight:

- Level Flight (Holding the constant altitude.)
- Step Climb (The fuel optimal altitude changes with decreasing weight of aircraft or actual environmental conditions (temperature, wind speed, etc.). Therefore, the FMS (Flight Management System) calculates the new fuel optimal altitude and the aircraft climbs to this new level where the flight is more effective. This procedure is called Step Climb.)
- Cruise Climb (Continuous climbing)

The Figure 1.2 shows currently climb techniques used in the cruise phase.

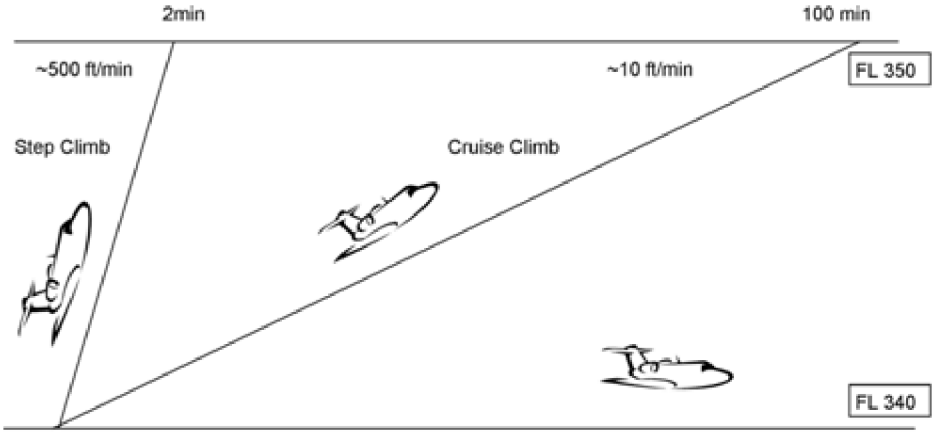

Figure 1.2: Difference between Level Flight, Step Climb and Cruise Climb

1.2 AIM OF THESIS

The purpose of this thesis is to validate the current Continuous Climbing Cruise simulation with the same simulation from the X-plane flight simulator. The fuel optimal Continuous Climbing Cruise is researched. The aims of the individual parts of the thesis are desired in this chapter.

For modeling of the vertical flight profile, some theoretical knowledge is necessary. A detailed theoretical framework of the equations of motion is introduced in chapter 2. The Taylor's series linearization technique is discussed in chapter 3. In the next part, the nonlinear aircraft model is built according to the equations of motion in chapter 4. The types of cruise flight are described in detail in chapter 5. Chapter 6 is focused on modification of the aircraft model by a time-varying mass parameter - the parameters of the aircraft model are set according to the Gulfstream G550.

The current Continuous Climbing Cruise is simulated and the fuel optimal Continuous Climbing Cruise is researched in the last part of the thesis. The longitudinal Auto Pilot and Auto Thrust for guidance of the aircraft model are proposed.

2. EQUATIONS OF MOTION

For understanding to the aircraft model and for following modeling of the vertical flight profile, some knowledge about the equations of motion for rigid body is needed. In this chapter, the equations of motion of an aircraft are derived and expressed in the state-space form; a summary of these state equations is given in section 2.4.

Several coordinate systems are used in aerospace applications. This thesis is limited on four coordinate systems: the body, the wind (the flight-path), the vehicle-carried vertical, and the topodetic coordinate system. These coordinate systems are described in appendix A.

2.1 GENERAL EQUATIONS OF MOTION

In the body-fixed reference frame, the linear and angular accelerations are represented by the six differential equations. For a rigid body the general force, moments, and angular momentum are resulted from these equations. These dependencies have been derived from Newton's laws. [1] [3]

The Figure 2.1 shows some physical components in relation to body-fixed reference frame. There are external forces and moments (F_x, F_y, F_z, L, M, and N) and linear and rotational velocity components (u, v, w, p, q, and r). The orientation of the flight-path axes in relation to the aircraft's body-axes is defined by an airspeed vector **V**, an angle of attack α, and a sideslip angle β.

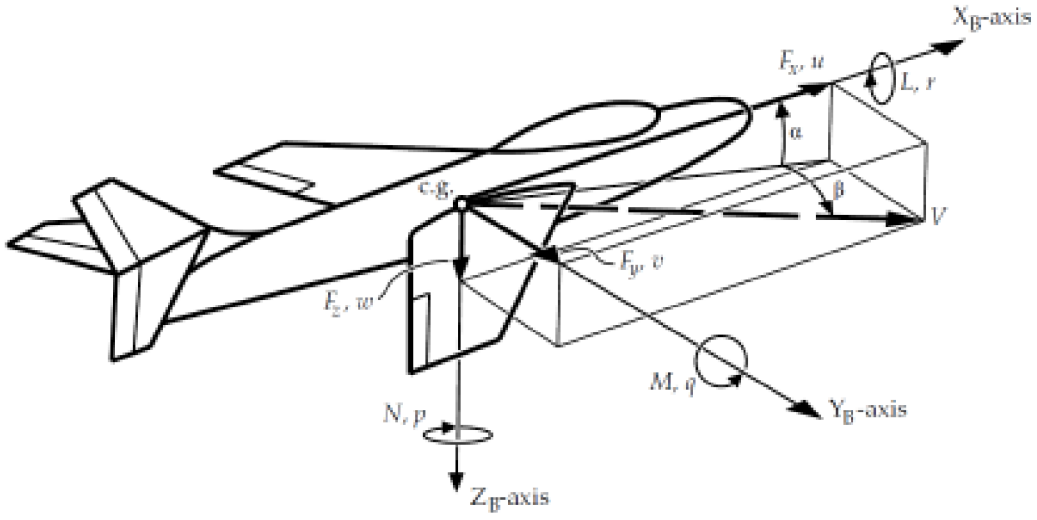

Figure 2.1: Orientation of the physical components in the Aircraft [1]

2.1.1 Force, Moment and Angular Momentum Equations for Rigid a Body

Consider an aircraft as a mass point $\delta\mathbf{m}$ with respect to center of gravity that moves with time-varying velocity **V** under the influence of external force **F**. Around the center of gravity is measured the external moment **M**, which is acting on an aircraft. This moment is equal to the time-derivative of the angular momentum of the mass point

relative. The equations for the total external force $\mathbf{F} = [F_x \; F_y \; F_z]^T$ and the external moment $\mathbf{M} = [L \; M \; N]^T$ becomes: [1] [3]

$$\mathbf{F} = m\dot{\mathbf{V}} \tag{2.1}$$

$$\mathbf{M} = \dot{\mathbf{h}} \tag{2.2}$$

where $\mathbf{V} = [u \; v \; w]^T$ is the velocity vector at the center of gravity, and **h** denotes the resulting angular momentum of the body. The angular momentum **h** is defined as a product of the inertia tensor of rigid body **I** with the angular velocity vector **Ω**. [1] [2]

$$\mathbf{h} = \mathbf{I} \cdot \mathbf{\Omega} \tag{2.3}$$

The angular velocity vector and inertia tensor of rigid body is defined for derive the angular momentum. The angular velocity $\mathbf{\Omega} = [p \; q \; r]^T$ is defined as sum of individual components p, q, and r (see Figure 2.1). [1]

$$\mathbf{\Omega} = \mathbf{i}p + \mathbf{j}q + \mathbf{k}r \tag{2.4}$$

where **i**, **j**, and **k** are unity vectors along the X, Y, and Z-axes. The inertia tensor of rigid body **I** is defined as: [1]

$$\mathbf{I} = \begin{bmatrix} I_{xx} & -J_{xy} & -J_{xz} \\ -J_{yx} & I_{yy} & -J_{yz} \\ -J_{zx} & -J_{zy} & I_{zz} \end{bmatrix} \tag{2.5}$$

The coefficients from this tensor are the moments and products of inertia of the rigid body. The coefficients of inertia tensor are depended upon the type of aircraft. If the airplane is symmetrical, J_{xy} and J_{yz} are both identically zero.

For an arbitrary position vector **r** with respect to the body reference frame we can then write: $\dot{\mathbf{r}} = \frac{\partial \mathbf{r}}{\partial t} + \Omega \times \mathbf{r}$ (2.6)

The equations (2.1) and (2.2) can be expanded by the equations (2.6). The vector-equations (2.7) and (2.8) are given by this application, which form the basis for the development of the general rigid-body dynamic model. The general external force and external moment equations: [2] [3]

$$\mathbf{F} = m\left(\frac{\partial \mathbf{V}}{\partial t} + \mathbf{\Omega} \times \mathbf{V}\right) \tag{2.7}$$

$$\mathbf{M} = \frac{\partial}{\partial t}(\mathbf{I} \cdot \mathbf{\Omega}) + \mathbf{\Omega} \times (\mathbf{I} \cdot \mathbf{\Omega}) \tag{2.8}$$

In order to make these equations usable for control system design and flight simulation, they need to be rewritten in nonlinear state-space format. This can be achieved by moving the time-derivatives of the linear and angular velocities to the left-hand side of these equations: [2]

$$\frac{\partial \mathbf{V}}{\partial t} = \frac{\mathbf{F}}{m} - \mathbf{\Omega} \times \mathbf{V} \tag{2.9}$$

$$\frac{\partial \boldsymbol{\Omega}}{\partial t} = \mathbf{I}^{-1}(\mathbf{M} - \boldsymbol{\Omega} \times \mathbf{I} \cdot \boldsymbol{\Omega}) \tag{2.10}$$

These vector-equations can be written into their components along the body-axes, according to Figure 2.1 for **V**, **Ω**, **F**, and **M**. There are time-derivatives components for velocity, which are used to in following chapter. [2]

$$\begin{aligned} \dot{u} &= \frac{F_x}{m} - qw + rv \\ \dot{v} &= \frac{F_y}{m} + pw - ru \\ \dot{w} &= \frac{F_z}{m} - pv + qu \end{aligned} \tag{2.11}$$

The angular velocity vector-equation (2.10) is rewritten into components of p, q, and r. These state equations are used to for build up the aircraft model. [1]

$$\begin{aligned} \dot{p} &= P_{pp}p^2 + P_{pq}pq + P_{pr}pr + P_{qq}q^2 + P_{qr}qr + P_{rr}r^2 + P_l L + P_m M + P_n N \\ \dot{q} &= Q_{pp}p^2 + Q_{pq}pq + Q_{pr}pr + Q_{qq}q^2 + Q_{qr}qr + Q_{rr}r^2 + Q_l L + Q_m M + Q_n N \\ \dot{r} &= R_{pp}p^2 + R_{pq}pq + R_{pr}pr + R_{qq}q^2 + R_{qr}qr + R_{rr}r^2 + R_l L + R_m M + R_n N \end{aligned} \tag{2.12}$$

The equations (2.11) and (2.12) are derived with assumptions as: the rotation and curvature of the Earth is neglected.

2.2 EXPRESSING TRANSLATIONAL MOTIONS IN FLIGHT-PATH AXES

In this chapter, the dynamics of aircraft in the flight-path (the wind) axes is described. It is more convenient to use an airspeed V, angle of attack α and sideslip angle β. There are variable expressions of the translational motions in relation to the flight-path axes. The exact terms of these variables in flight-path axes are shown in the appendix A.

The components of the body-axes velocity are equal to (see Figure 2.1): [1]

$$\begin{bmatrix} u \\ v \\ w \end{bmatrix} = V \begin{bmatrix} \cos\alpha\cos\beta \\ \sin\beta \\ \sin\alpha\cos\beta \end{bmatrix} \tag{2.13}$$

Hence:

$$\begin{aligned} V &= \sqrt{u^2 + v^2 + w^2} \\ \alpha &= \arctan\left(\frac{w}{u}\right) \\ \beta &= \arctan\left(\frac{v}{\sqrt{u^2 + w^2}}\right) \end{aligned} \tag{2.14}$$

Differentiation of the equations (2.14) with respect to the time and substituting the equations (2.11) and (2.13) yields: [1] [2]

$$\dot{V} = \frac{1}{m}(F_x \cos\alpha\cos\beta + F_y \sin\beta + F_z \sin\alpha\cos\beta)$$

$$\dot{\alpha} = \frac{1}{V\cos\beta}\left\{\frac{1}{m}(-F_x \sin\alpha + F_z \cos\alpha)\right\} + q - (p\cos\alpha + r\sin\alpha)\tan\beta$$

$$\dot{\beta} = \frac{1}{V}\left\{\frac{1}{m}(-F_x \cos\alpha\sin\beta + F_y \cos\beta - F_z \sin\alpha\sin\beta)\right\} + p\sin\alpha - r\cos\alpha \tag{2.15}$$

2.3 KINEMATIC RELATIONS

The differential equations for the airspeed, angle of attack, sideslip angle, and the rotational velocity components have been derived. For the following work, the flight path relative to the Earth is needed. The orientation of the aircraft relative to the Earth is given by a series of three consecutive rotations, the Euler angles ψ, θ, and φ, see appendix A.

It is possible to express the total angular velocity of an aircraft expressed in terms of the derivatives with respect to time of the Euler angles: [1] [2]

$$\begin{bmatrix} p \\ q \\ r \end{bmatrix} = \begin{bmatrix} 1 & 0 & -\sin\theta \\ 0 & \cos\varphi & \sin\varphi\cos\theta \\ 0 & -\sin\varphi & \cos\varphi\cos\theta \end{bmatrix} \begin{bmatrix} \dot{\varphi} \\ \dot{\theta} \\ \dot{\psi} \end{bmatrix} \tag{2.16}$$

where the angular velocities are transformed by this matrix from the Earth-fixed axis system into body-axes angular velocities. The time-derivatives of the Euler angles are found by multiplying the angular velocities with inverse matrix. The kinematic relation is:

$$\dot{\psi} = \frac{q\sin\varphi + r\cos\varphi}{\cos\theta}$$

$$\dot{\theta} = q\cos\varphi - r\sin\varphi$$

$$\dot{\varphi} = p + (q\sin\varphi + r\cos\varphi)\tan\theta \tag{2.17}$$

The last point is defined the position of the aircraft with respect to the Earth. The equations are defined conversion from Earth-fixed axes system to body-axes system: [1]

$$\dot{x}_e = \{u_e\cos\theta + (v_e\sin\varphi + w_e\cos\varphi)\sin\theta\}\cos\psi - (v_e\cos\varphi - w_e\sin\varphi)\sin\psi$$

$$\dot{y}_e = \{u_e\cos\theta + (v_e\sin\varphi + w_e\cos\varphi)\sin\theta\}\sin\psi + (v_e\cos\varphi - w_e\sin\varphi)\cos\psi$$

$$\dot{z}_e = -u_e\sin\theta + (v_e\sin\varphi + w_e\cos\varphi)\cos\theta \tag{2.18}$$

2.4 STATE EQUATIONS

In this chapter, all state equations are summarized for build up main part of the nonlinear state-space model. First six differential equations represent the linear and angular velocities of the aircraft. These equations were derived from the basic force and moment equations (see section 2.1 and 2.2).

$$\dot{V} = \frac{1}{m}(F_x \cos\alpha\cos\beta + F_y \sin\beta + F_z \sin\alpha\cos\beta)$$

$$\dot{\alpha} = \frac{1}{V\cos\beta}\left\{\frac{1}{m}(-F_x \sin\alpha + F_z \cos\alpha)\right\} + q - (p\cos\alpha + r\sin\alpha)\tan\beta$$

$$\dot{\beta} = \frac{1}{V}\left\{\frac{1}{m}(-F_x \cos\alpha\sin\beta + F_y \cos\beta - F_z \sin\alpha\sin\beta)\right\} + p\sin\alpha - r\cos\alpha$$

$$\dot{p} = P_{pp}p^2 + P_{pq}pq + P_{pr}pr + P_{qq}q^2 + P_{qr}qr + P_{rr}r^2 + P_l L + P_m M + P_n N$$

$$\dot{q} = Q_{pp}p^2 + Q_{pq}pq + Q_{pr}pr + Q_{qq}q^2 + Q_{qr}qr + Q_{rr}r^2 + Q_l L + Q_m M + Q_n N$$

$$\dot{r} = R_{pp}p^2 + R_{pq}pq + R_{pr}pr + R_{qq}q^2 + R_{qr}qr + R_{rr}r^2 + R_l L + R_m M + R_n N \tag{2.19}$$

Additional six state equations are the equations for the Euler angles and the positions of the aircraft (altitude and horizontal coordinates) relative to the Earth. These equations are needed for practical purposes and determine the aerodynamic, propulsive, etc. force and moment.

$$\dot{\psi} = \frac{q\sin\varphi + r\cos\varphi}{\cos\theta}$$

$$\dot{\theta} = q\cos\varphi - r\sin\varphi$$

$$\dot{\varphi} = p + (q\sin\varphi + r\cos\varphi)\tan\theta$$

$$\dot{x}_e = \{u_e\cos\theta + (v_e\sin\varphi + w_e\cos\varphi)\sin\theta\}\cos\psi - (v_e\cos\varphi - w_e\sin\varphi)\sin\psi$$

$$\dot{y}_e = \{u_e\cos\theta + (v_e\sin\varphi + w_e\cos\varphi)\sin\theta\}\sin\psi + (v_e\cos\varphi - w_e\sin\varphi)\cos\psi$$

$$\dot{H} = -u_e\sin\theta + (v_e\sin\varphi + w_e\cos\varphi)\cos\theta \tag{2.20}$$

Complete state vector is $x = [V \;\; \alpha \;\; \beta \;\; p \;\; q \;\; r \;\; \psi \;\; \theta \;\; \varphi \;\; x_e \;\; y_e \;\; H]^T$. These equations form the core (so-called Equations of Motions) of the aircraft model. The equations are combined in a nonlinear state-space system: [1]

$$\dot{\mathbf{x}} = f'(\mathbf{x}, \mathbf{F}_{tot}(t), \mathbf{M}_{tot}(t)) \tag{2.21}$$

where input vector are:

$$\mathbf{F}_{tot}(t) = g_1(\mathbf{x}(t), \mathbf{u}(t), \mathbf{v}(t), t) \tag{2.22}$$

$$\mathbf{M}_{tot}(t) = g_2(\mathbf{x}(t), \mathbf{u}(t), \mathbf{v}(t), t) \tag{2.23}$$

The body-axes components of external forces and moments are the input variables of this system, while the body-axes components of linear and rotational velocities can be regarded as the state variables of this system.

By inserting of the equations (2.22) and (2.23) into (2.21) gives now the nonlinear state-space system: [1]

$$\dot{\mathbf{x}}(t) = f(\mathbf{x}(t), \mathbf{u}(t), \mathbf{v}(t), t) \tag{2.24}$$

with state vector **x**, input vector **u**, disturbance vector **v**, and time t. The complete aircraft model is formed by this nonlinear state-space system (2.24). In the next chapter, a dynamic aircraft model is built on this foundation.

3. LINEARIZATION STATE EQUATIONS

In this chapter, the theoretical background about linearization has been described. The linear state equations are derived via Taylor series. This theoretical background can help reader to understand problems about linearization, which are discussed in the chapter 7.

3.1 LINEARIZATION VIA TAYLOR SERIES

In order to linearization of the nonlinear state-space system, there is shown the Taylor Series expansion of functions. The Taylor Series expansion of f(x) around the point $\bar{x}$ is given by (3.1):

$$f(x) = f(\bar{x}) + \left.\frac{\partial f}{\partial x}\right|_{x=\bar{x}} (x - \bar{x}) + \textit{higher order terms} \tag{3.1}$$

Consider the nonlinear state-space system:

$$\begin{aligned} \dot{\mathbf{x}}(t) &= \mathbf{f}\big(\mathbf{x}(t), \mathbf{u}(t)\big) \\ \mathbf{y}(t) &= \mathbf{g}\big(\mathbf{x}(t), \mathbf{u}(t)\big) \end{aligned} \tag{3.2}$$

The equations (3.2) can be expanded in a Taylor-series about an equilibrium point ($\mathbf{x}_0$, $\mathbf{u}_0$). The higher order terms are neglected, and equations become: [1]

$$\begin{aligned} \dot{\mathbf{x}} - \dot{\mathbf{x}}_0 &\approx \frac{\partial \mathbf{f}}{\partial \mathbf{x}}\big(\mathbf{x} - \mathbf{x}_0\big) + \frac{\partial \mathbf{f}}{\partial \mathbf{u}}\big(\mathbf{u} - \mathbf{u}_0\big) \\ \mathbf{y} - \mathbf{y}_0 &\approx \frac{\partial \mathbf{g}}{\partial \mathbf{x}}\big(\mathbf{x} - \mathbf{x}_0\big) + \frac{\partial \mathbf{g}}{\partial \mathbf{u}}\big(\mathbf{u} - \mathbf{u}_0\big) \end{aligned} \tag{3.3}$$

where $\dot{\mathbf{x}}_0 = \mathbf{f}\big(\mathbf{x}_0, \mathbf{u}_0\big)$, $\mathbf{y}_0 = \mathbf{g}\big(\mathbf{x}_0, \mathbf{u}_0\big)$ and partial derivative matrices are determined for operating point $\big(\mathbf{x}_0, \mathbf{u}_0\big)$.

Now define: [1]

$$\begin{aligned} \mathbf{x}' &= \mathbf{x} - \mathbf{x}_0 \\ \mathbf{y}' &= \mathbf{y} - \mathbf{y}_0 \\ \mathbf{u}' &= \mathbf{u} - \mathbf{u}_0 \end{aligned} \tag{3.4}$$

and:

$$\begin{aligned} A &= \left.\frac{\partial \mathbf{f}}{\partial \mathbf{x}}\right|_{(\mathbf{x_0}, \mathbf{u_0})} & C &= \left.\frac{\partial \mathbf{g}}{\partial \mathbf{x}}\right|_{(\mathbf{x_0}, \mathbf{u_0})} \\ B &= \left.\frac{\partial \mathbf{f}}{\partial \mathbf{u}}\right|_{(\mathbf{x_0}, \mathbf{u_0})} & D &= \left.\frac{\partial \mathbf{g}}{\partial \mathbf{u}}\right|_{(\mathbf{x_0}, \mathbf{u_0})} \end{aligned} \tag{3.5}$$

By the substitution into equation (3.3), the linear state-space system is obtained: [1]

$$\begin{aligned} \dot{\mathbf{x}}' &= A\mathbf{x}' + B\mathbf{u}' \\ \mathbf{y}' &= C\mathbf{x}' + D\mathbf{u}' \end{aligned} \tag{3.6}$$

The operating point ($\mathbf{x}_0$, $\mathbf{u}_0$) is chosen to be a singular point or equilibrium point. By using the suitable operating point and theoretical knowledge above, the linear state-space system is obtained. [1]

The complete system matrices (A, B, C, D) are defined: [1]

$$\begin{aligned} A &= (n \times n) & C &= (m \times n) \\ B &= (n \times m) & D &= (m \times m) \end{aligned} \tag{3.7}$$

where n states and m observation variables.

4. AIRCRAFT MODEL

The nonlinear aircraft model is described in this chapter. The aircraft model is constructed according to state equations of motions hereinbefore. The first outline is the general structure of the aircraft model, further are identification of the individual contributions to the forces, moments and the necessary airdata equations. The aircraft dynamics is defined by these equations. The aircraft model is used to for simulation the Continuous Climbing Cruise.

4.1 GENERAL STRUCTURE OF MODEL

The general structure of aircraft model is founded on the nonlinear state-space system (2.21). The block-diagram of aircraft model is shown in the Figure 4.1. All elements from this figure represent the system (2.21). The equations of motion are main part of the aircraft model. The other part is determined by the external forces and moments. For completing model, $\mathbf{F_{tot}}$ and $\mathbf{M_{tot}}$ are needed (see equation 2.21). Those external control inputs are defined by aerodynamics, propulsion, gravity, and wind forces and moments.

The state variables are obtained by integrating their time-derivatives with respect to time, taking into account the initial value of the state vector, $\mathbf{x_0}$. All forces and moments must be expressed in components along the body-axes of the aircraft. If it doesn't, the forces and moments must be transformed to body-axes components (e.g. transformation of aerodynamic forces and moments from the flight-path axes to body axes).[1]

The complete aircraft model is formed according to the Figure 4.1, where input vector **u** is defined by components for aerodynamics, propulsion, and wind. There are aerodynamic inputs $\mathbf{u}_{aero} = [\delta_e\ \delta_a\ \delta_r\ \delta_f]^T$, propulsion inputs $\mathbf{u}_{prop} = [F_{xp}\ F_{yp}\ F_{zp}\ L_p\ M_p\ N_p]^T$ and wind inputs $\mathbf{u}_{wind} = [u_w\ v_w\ w_w\ \dot{u}_w\ \dot{v}_w\ \dot{w}_w]^T$. The input vector $\mathbf{u}_{aero}$ gathers the positions of the elevator, ailerons, and rudder (the primary flight controls of aircraft), and flaps (the secondary flight controls). The output vector is equal state vector $\mathbf{x} = [V\ \alpha\ \beta\ p\ q\ r\ \psi\ \theta\ \varphi\ x_e\ y_e\ H]^T$.

4.2 EXTERNAL FORCES AND MOMENTS

In this chapter, the different contributions to the external forces and moments are identified. Those contributions are depended on the type of aircraft. There are the forces and moments which are considered:

- The aerodynamic forces and moments
- The propulsive forces and moments
- The gravitational forces
- The wind forces

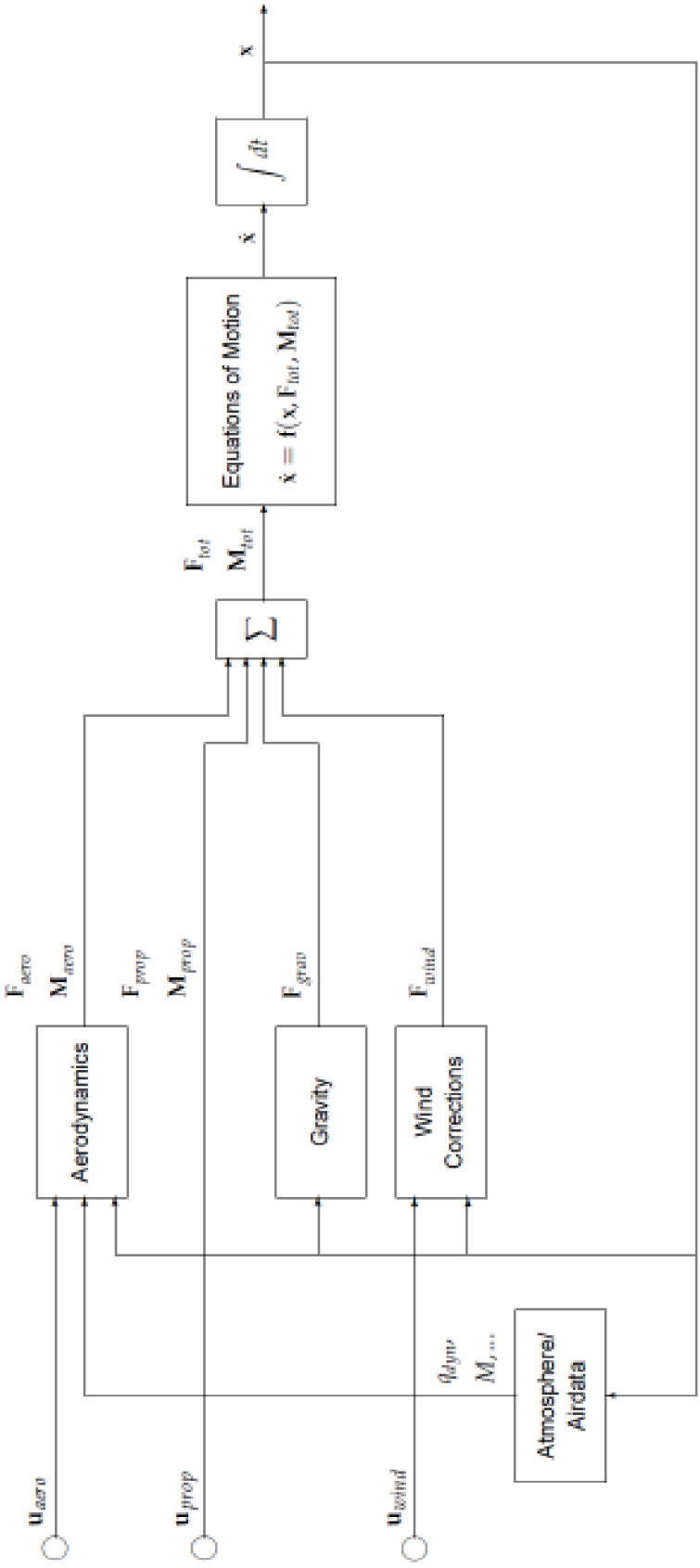

Figure 4.1: Block diagram of the General Aircraft Model [1]

The total external forces $\mathbf{F}_{tot}$ and moments $\mathbf{M}_{tot}$ are determined by the sum of all contributions to the external forces and moments.

Resulting total forces then become:

$$\mathbf{F}_{tot} = \mathbf{F}_{aero} + \mathbf{F}_{prop} + \mathbf{F}_{grav} + \mathbf{F}_{wind} \tag{4.1}$$

Resulting total moments then become:

$$\mathbf{M}_{tot} = \mathbf{M}_{aero} + \mathbf{M}_{prop} \tag{4.2}$$

where $\mathbf{F}_{aero}, \mathbf{F}_{prop}, \mathbf{F}_{grav}, \mathbf{F}_{wind}, \mathbf{M}_{aero}\ \mathbf{M}_{prop}$ represent all forces and moments, acting on the aircraft. The components of forces and moments are determined by the following vectors:

The aerodynamic forces and moments

$$\mathbf{F}_{aero} = \left[F_{X\,a}\ F_{Y\,a}\ F_{Z\,a}\right] \tag{4.3}$$

$$\mathbf{M}_{aero} = \left[L_a\ M_a\ N_a\right]$$

The propulsive forces and moments

$$\mathbf{F}_{prop} = \left[F_{X\,p}\ F_{Y\,p}\ F_{Z\,p}\right] \tag{4.4}$$

$$\mathbf{M}_{prop} = \left[L_p\ M_p\ N_p\right]$$

The gravitational forces

$$\mathbf{F}_{grav} = \left[F_{X\,gr}\ F_{Y\,gr}\ F_{Z\,gr}\right] \tag{4.5}$$

The wind forces

$$\mathbf{F}_{wind} = \left[F_{X\,w}\ F_{Y\,w}\ F_{Z\,w}\right] \tag{4.6}$$

There are listed the equations to determine the individual components of total external forces $\mathbf{F}_{tot} = [F_X\ F_Y\ F_Z]$ and moments $\mathbf{M}_{tot} = [L\ M\ N]$ along the body-axes.

Resulting forces along the body-axes, [N]:

$$\begin{aligned} F_x &= F_{X\,a} + F_{X\,p} + F_{X\,gr} + F_{X\,w} \\ F_y &= F_{Y\,a} + F_{\dot{Y}\,p} + F_{Y\,gr} + F_{Y\,w} \\ F_z &= F_{Z\,a} + F_{Z\,p} + F_{Z\,gr} + F_{Z\,w} \end{aligned} \tag{4.7}$$

Resulting moments around the body-axes, [Nm]:

$$\begin{aligned} L &= L_a + L_p \\ M &= M_a + M_p \\ N &= N_a + N_p \end{aligned} \tag{4.8}$$

The vertical flight profile is assumed, therefore the sideforce (F_y), roll (L), and yaw (N) moment are not considered. The total external force along the Y_B-axis is zero. The total external moments roll and yaw around the X_B and Z_B-axis are also zero. The individual forces and moments are explained below.

4.2.1 Aerodynamics Forces and Moment

The aerodynamic forces and moment acting upon the aircraft are lift, drag and pitching moment as shows the Figure 4.2. The aerodynamic forces and moment depend on the several factors, which are described thereinafter.

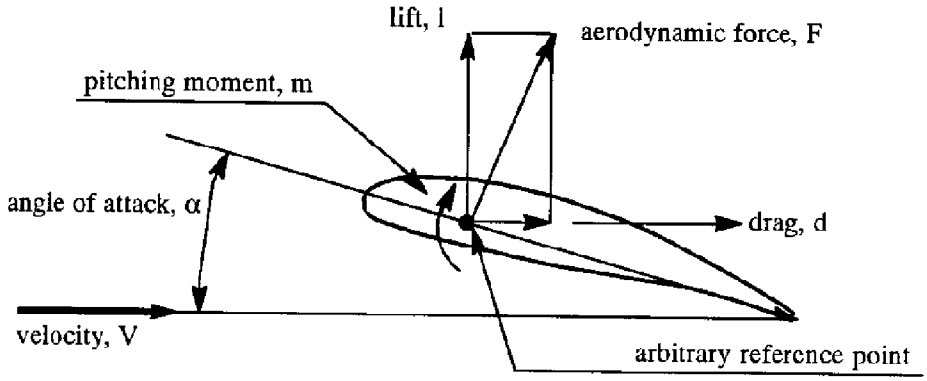

Figure 4.2: Definition of the section (Aerofoil) forces and moment [4]

Lift Force

Lift force is generated by each part of the aircraft, but main component is generated by the wings. Aircraft lift force acts through a single point called the center of pressure. The center of pressure is defined just like the center of gravity, but using the pressure distribution around the body, instead of the weight distribution. [6] [20]

Lift force is affected by these main factors:

- the angle of attack
- the shape of the wing — the aerofoil
- the density of the air
- the flight airspeed
- the wing plan-form surface area.

There is a standard equation to calculate lift force: [4]

$$L = \frac{1}{2} C_L \rho V^2 S \qquad (4.8)$$

where ρ is density of air (kg/m^3), V is the true airspeed (m/s), S is the wing area (m^2), C_L is the lift coefficient.

The C_L is dimensionless lift coefficient, which expresses the lift force generated by an aircraft. The lift coefficient contains all complex dependencies and it is usually determined experimentally. The lift coefficient is defined by the more simple equation (4.9). There is assumed the dependence on the angle of attack and the aerofoil:

$$C_L = C_{L_0} + C_{L_\alpha} \alpha \qquad (4.9)$$

In the history, most of aircraft manufactures has developed and tested many series of airfoils. Some of them are used until nowdays. Figure 4.3 shows the relation between lift coefficient and angle of attack.

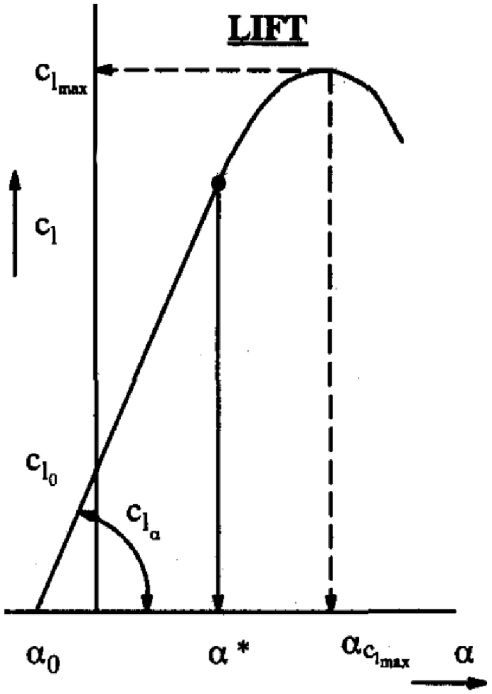

Figure 4.3: Lift coefficient vs. Angle of attack [3]

Drag Force

Drag force is the air resistance to aircraft and due to this it is pushing on the aircraft. Drag force is directed along and opposite to the flight direction. In the same way like the lift, drag is acting on the aircraft's center of pressure. [7]

Drag force is affected by these main factors:

- the angle of attack
- the streamlining of the aircraft body
- the density of the air
- the speed of the airflow

There is a standard equation to calculate drag force: [4]

$$D = \frac{1}{2} C_D \rho V^2 S \qquad (4.10)$$

where C_D is dimensionless drag coefficient which expresses air resistance to aircraft during the aircraft movement in air. The drag coefficient contains all complex dependencies and is usually determined experimentally. The drag coefficient is defined by the simplified equation (4.11). There is assumed dependence on the lift coefficient and flow condition:

$$C_D = C_{D_0} + \frac{C_L^2}{\pi \cdot AR \cdot e} \tag{4.11}$$

The total drag is composited from the induced drag and the parasite drag as shows Figure 4.4.

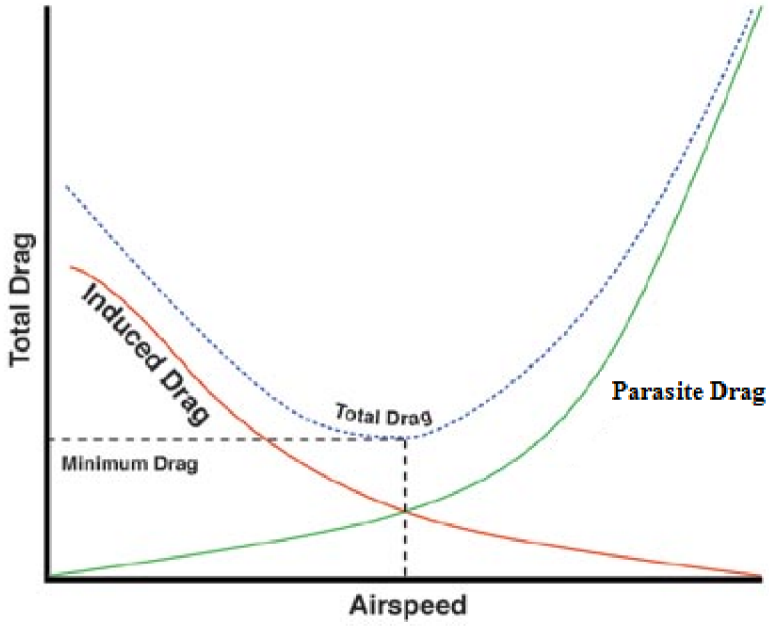

Figure 4.4: Drag force vs. Airspeed [23]

The parasitic drag comprises from contributions of wings, tail surfaces, fuselage, and landing gear. The parasitic drag is expressed by the coefficient C_{D0}. The lift induced drag is caused by change of the airflow speed and direction behind the trailing edge. The induced draft is depended on the lift coefficient C_L and on the constant aircraft wing dimensions. [6] [7]

Lift to Drag Ratio

Lift to drag ratio is considered as a factor of aerodynamic efficiency of the aircraft. The aircraft has a high L/D ratio if it is produced a large lift force or a small drag force.

During the cruise phase, the lift force is equal to the weight force. A high lift aircraft can carry a more payload. The thrust force is equal to drag force. With a low drag the low thrust is required and therefore lower fuel consumption can be achieved. Both forces are dependent on the angle of attack (see Figure 4.5). In order to achieve the optimal flight conditions the L/D ratio should be maximized. [21]

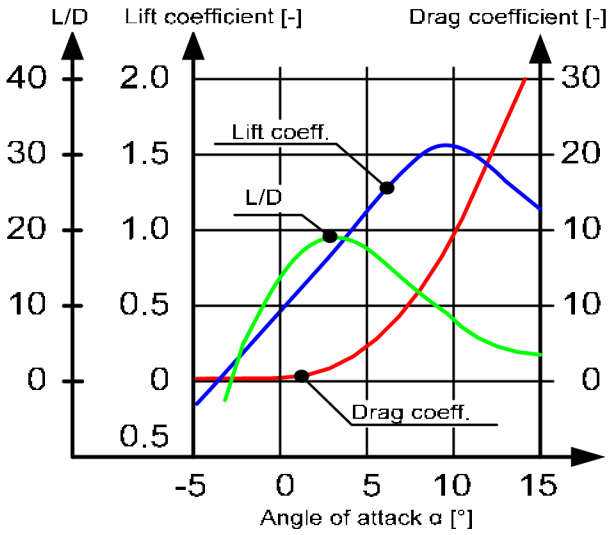

Figure 4.5: Dependence of Lift and Drag coefficient upon Angle of attack [17]

Pitching Moment

The pitching motion is caused by the deflection of the elevator of the aircraft. The change in lift created by deflection elevator generates a pitching moment around the aerodynamic centre of the wing and body.

There is a standard equation to calculate pitching moment: [4]

$$M_a = \frac{1}{2} C_m \rho V^2 S\bar{c} \tag{4.12}$$

where $\bar{c}$ is the mean aerodynamic chord (m) and C_M is the pitching coefficient. The C_M is dimensionless pitching coefficient which expresses the pitching moment generated by an aircraft to rotate. There is assumed dependence on the angle of attack, pitch rate, and elevator deflection: [4]

$$C_M = C_{m_\alpha}\alpha + C_{m_q}\frac{q\bar{c}}{V} + C_{m_{\delta_e}}\delta_e \tag{4.13}$$

Summary

The model express aerodynamic forces along the aircraft's flight-path and pitching moment along the aircraft's body-axes in these equations:

Aerodynamic forces, [N]:

$$D = \frac{1}{2} C_D \rho V^2 S \tag{4.14}$$

$$L = \frac{1}{2} C_L \rho V^2 S \tag{4.15}$$

Aerodynamic moment, [Nm]:

$$M_a = \frac{1}{2} C_m \rho V^2 S\bar{c} \tag{4.16}$$

The aerodynamic forces and moment depend on the flight condition, defined by the state vector x, control inputs defined by the input vector $\mathbf{u}_{aero} = [\delta_e\ \delta_a\ \delta_r\ \delta_f]^T$, and the type of the aircraft.

The aerodynamic forces must be transformed to body-axes components. The relationship between aerodynamic forces in flight-path and body-axes shows in Figure 4.6.

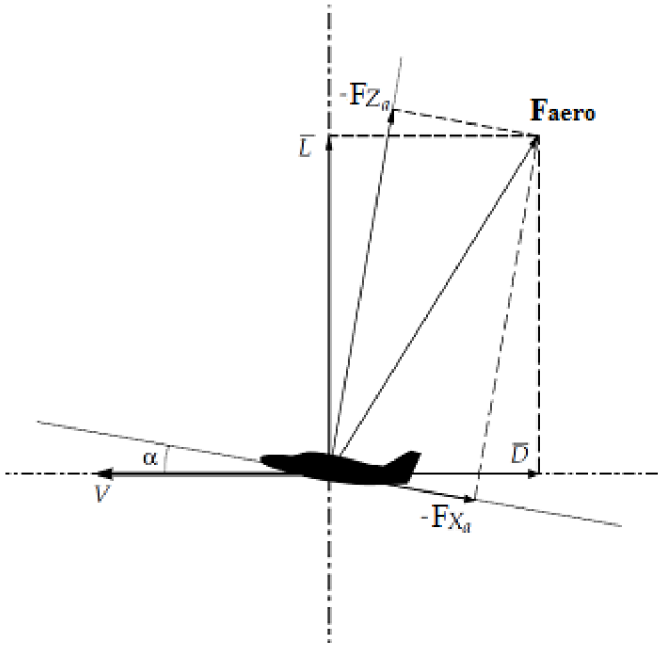

Figure 4.6: The aerodynamic forces in Flight-path and Body-axes [1]

The body-axes components of aerodynamic forces are defined by: [1]

$$F_{X\,a} = L\sin\alpha - D\cos\alpha$$
$$F_{Z\,a} = -L\cos\alpha - D\sin\alpha \qquad (4.17)$$

The final vectors of aerodynamic forces and moments are represented by these equations:

$$\mathbf{F}_{aero} = \left[F_{X\,a}\ 0\ F_{Z\,a}\right] \qquad (4.18)$$

$$\mathbf{M}_{aero} = \left[0\ M_a\ 0\right] \qquad (4.19)$$

4.2.2 Propulsive Forces and Moments

To the drag overcoming, the aircrafts are using a propulsion system to generate a force called thrust. The magnitude of the thrust depends on many factors associated with the propulsion system including throttle control and flight condition like is the altitude and Mach number. [6] [8]

There is a standard equation for thrust calculation:

$$T = \frac{1}{2} C_T \rho V^2 S \qquad (4.20)$$

where C_T is a function of power/throttle setting, fuel flow rate, blade angle, Mach number and other parameters.

The propulsive forces and moments are represented by the input $\mathbf{u}_{prop} = [F_{xp}\ F_{yp}\ F_{zp}\ L_p\ M_p\ N_p]^T$. The component of propulsive force along X-axis is only considered. The other forces and moments are neglected. The body-axes component of propulsive force along X-axis is defined by the equations:

$$F_{X_p} = T \tag{4.21}$$

The final vectors of propulsive forces and moments are represented by these equations:

$$\mathbf{F}_{prop} = [T\ 0\ 0] \tag{4.22}$$

$$\mathbf{M}_{prop} = [0\ 0\ 0] \tag{4.23}$$

Now there is further basic performance described briefly and engine which is used in the Gulfstream G550. The Gulfstream G550 is the long range business jet aircraft with two turbofan engine.

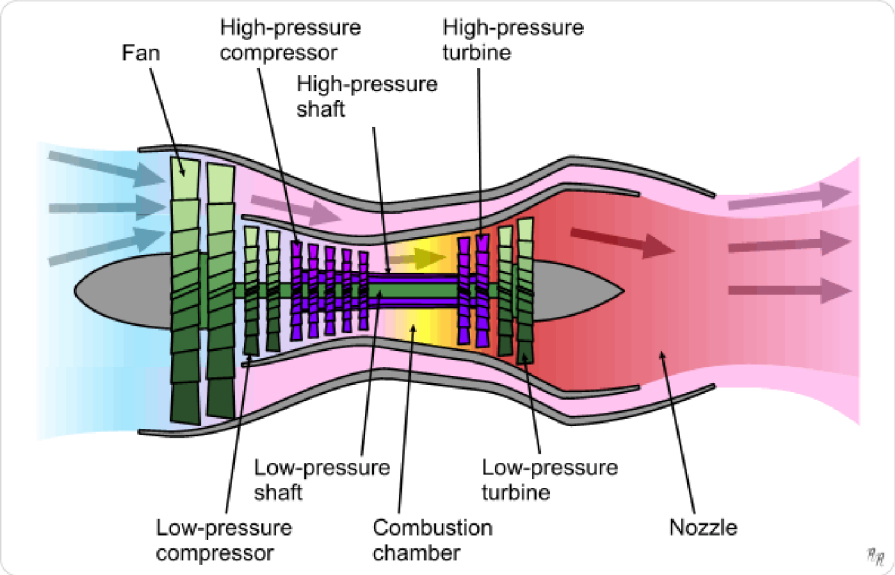

Figure 4.7: The general structure of the Turbofan Engine [10]

The air enter into the high-pressure compressor, where the temperature and pressure of the air is increased. This compression is necessary for the fuel combustion. In the combustion chamber, the fuel and air are ignited. There are released large amounts of energy. The combustion gases enter the turbine. The turbine can be divided by high-pressure and low-pressure turbine. High-pressure turbine transforms the energy of the combustion gases into rotational energy for the high-pressure compressor, which is connected through shaft with high-pressure turbine. The low-pressure turbine transforms the energy of the combustion gases into rotational energy for the fan. After the combustion gases exhaust from low-pressure turbine, they enter the nozzle inlet. The nozzle transforms the gases 'remaining energy into thrust at the nozzle exit. [9]

4.2.3 Gravitational Forces

The weight of the aircraft equals the aircraft's mass m times the local acceleration of gravity **g**. The vector of acceleration of gravity is defined in the vehicle-carried vertical

reference system. The gravitational forces are needed in the body-axes. The gravity force components along the aircraft's body-axes are founded on the following equation: [1]

$$\begin{aligned} F_{X\,gr} &= -mg \cdot \sin\theta \\ F_{Y\,gr} &= mg \cdot \cos\theta \sin\varphi \\ F_{Z\,gr} &= mg \cdot \cos\theta \cos\varphi \end{aligned} \qquad (4.24)$$

where g is the magnitude of the local acceleration of gravity, θ is the pitch angle of the aircraft, and φ is the roll angle of the aircraft.

The weight force is presumed to acting from the aircrafts centre of gravity (c.g) to the centre of the Earth. The position of c.g within the aircraft is varying according to the seating, luggage stowage and fuel distribution in the tanks. The weight of the aircraft decreases during the flight as the fuel is burned. [6]

The final vector of gravitational forces is represented by this equation:

$$\mathbf{F}_{grav} = \left[F_{Xgr}\ F_{Ygr}\ F_{Zgr}\right] \qquad (4.25)$$

4.2.4 Wind Forces

The wind forces are considered as last contribution into the all forces, because the aircraft is flying in nonsteady atmosphere. The equations for wind forces are equal to: [1]

$$\begin{aligned} F_{X\,w} &= -m \cdot \left(\dot{u}_w + qw_w - rv_w\right) \\ F_{Y\,w} &= -m \cdot \left(\dot{v}_w - pw_w + ru_w\right) \\ F_{Z\,w} &= -m \cdot \left(\dot{w}_w + pv_w - qu_w\right) \end{aligned} \qquad (4.26)$$

The wind forces depend on the flight condition, defined by the state vector x, and the control inputs, defined by the input vector $\mathbf{u}_{wind} = [u_w\ v_w\ w_w\ \dot{u}_w\ \dot{v}_w\ \dot{w}_w]^T$.

The final vector of wind forces is represented by this equation:

$$\mathbf{F}_{wind} = \left[F_{Xw}\ F_{Yw}\ F_{Zw}\right] \qquad (4.27)$$

4.3 AIRDATA VARIABLES

In order to express the aerodynamic forces and moment in terms of dimensional force, some of airdata variables are needed. There are requirement knowledge of the dynamic pressure and variables related to its. These variables are closely related to the properties of the atmosphere, and the airspeed and altitude of the aircraft. [1]

The dynamic pressure q_{dyn} are functions of change of airspeed and air density:

$$q_{dyn} = \frac{1}{2}\rho V^2 \qquad \text{[Pa]} \qquad (4.28)$$

In the aircraft model, the value of dynamic pressure is counted according to the ICAO Standard Atmosphere model.

5. TYPES OF CRUISE FLIGHTS

In this chapter, the types of cruise flight are described. The brief description was written in the Introduction (see Figure 1.2). To learn more about the cruise flights, we look at again the forces acting on the aircraft during a steady symmetrical flight. The Figure 5.1 provides a definition of all forces. The individual forces aren't defined here.

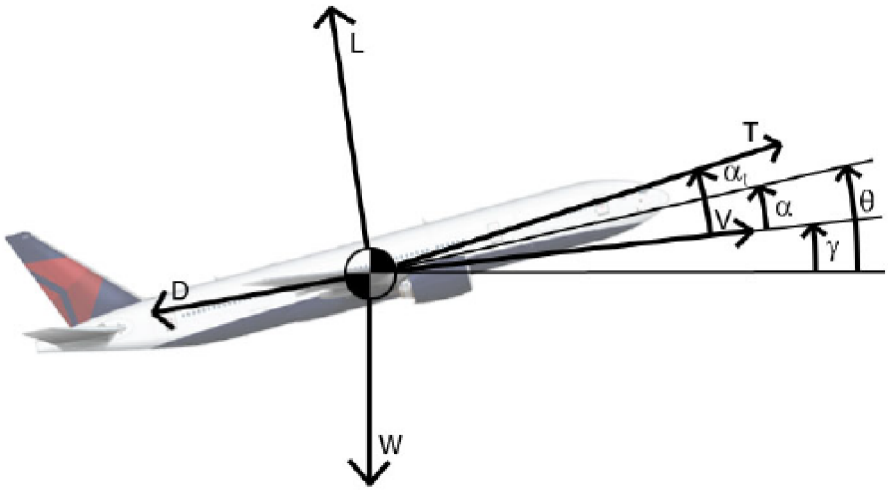

Figure 5.1: The forces acting on the Aircraft [22]

More information about lift L, drag D, weight W, and thrust T has been written in the section 4.2. The Figure 5.1 shows the flight path angle γ, the angle of attack α, and the pitch angle θ. The thrust angle of attack ($\alpha_t = 0$) is not considered, so the thrust points in the direction of the velocity. There is important relationship between angles:

$$\theta = \alpha + \gamma \tag{5.1}$$

There are simple equations of motion, which are defined by the second Newton's law. These equations are same as the state equation of motion from the section 2.4. But there are described only balance of forces acting upon aircraft and linear velocities. These equations can help to describe aircraft behavior in each type of the cruise flight.

Forces in vertical and horizontal components: [22]

$$m\frac{dV}{dt} = T - D - W\sin\gamma \tag{5.2}$$

$$mV\frac{d\gamma}{dt} = L - W\cos\gamma \tag{5.3}$$

Vertical and horizontal velocities: [22]

$$\frac{dH}{dt} = V\sin\gamma \tag{5.4}$$

$$\frac{ds}{dt} = V\cos\gamma \tag{5.5}$$

5.1 LEVEL FLIGHT

In the level flight, the aircraft is controlled by actuators, according to flight plan upon the defined altitude all flight time. In this type of cruise flight, the aerodynamic lift is reduced. Lift is decreased by the actuator. The conditions limiting the level flight are shown in the Table 5.1.

Flight Altitude	Constant
Dynamic pressure	Constant
Airspeed	Constant
Flight path angle	Zero

Table 5.1: Description of the variable settings in the Level Flight

Combining these conditions with the equations (5.2), (5.3) above gives: [22]

$$0 = T - D \quad \Rightarrow \quad T = D \tag{5.6}$$

$$0 = L - W \quad \Rightarrow \quad L = W \tag{5.7}$$

and vertical respective horizontal velocities: [22]

$$\frac{dH}{dt} = 0 \tag{5.8}$$

$$\frac{ds}{dt} = V \tag{5.9}$$

5.2 STEP CLIMB

The step climb technique is one of methods of fuel saving, which are currently used. If the step climb is need, the flight level changes. The aircraft is climbed until new flight level is achieved. This maneuver is repeated in fixed steps, because an aircraft still establish efficient cruise altitudes. The conditions limiting the step climb are shown in the Table 5.2. [22]

Flight Altitude	Inconstant
Dynamic pressure	Constant
Airspeed	Constant
Flight path angle	Constant

Table 5.2: Description of the variable settings in the Step Climb

Combining these conditions with the equations (5.2), (5.3) above gives: [22]

$$\sin\gamma = \frac{T - D}{W} \tag{5.10}$$

$$\cos\gamma = \frac{L}{W} \tag{5.11}$$

and vertical respective horizontal velocities: [22]

$$\frac{dH}{dt} = \frac{T - D}{W} V \tag{5.12}$$

$$\frac{ds}{dt} = V \frac{L}{W} \tag{5.13}$$

5.3 CRUISE CLIMB

The cruise climb is defined as a continuous climb in the cruise flight that optimizes the vertical profile with respect to fuel consumption. The aircraft altitude is continually increased to ensure that the aircraft is at optimum altitude as its weight decreases due to fuel consumption. The weight of the aircraft decreases during flight, according to: [22]

$$\frac{dW}{dt} = -FF(V, H, \Gamma) \tag{5.14}$$

where FF is the fuel flow, which depends on the velocity V, the height H and the engine setting Γ.

The cruise climb is achieved by setting the aircraft to level flight and the vertical control is turned off. The gravitational force is decreased on the other side the aerodynamic lift is increased. The altitude is increased without controls. The cruise climb continues until the vertical control is turned on (or until atmosphere/fuel conditions allows so). The increase in altitude should be proportional to weight loss in order to keep force equilibrium.

Combining these conditions with the equations above gives: [22]

$$T = D \tag{5.15}$$

$$L > W \tag{5.16}$$

and vertical respective horizontal velocities: [22]

$$\frac{dH}{dt} = 0 \tag{5.17}$$

$$\frac{ds}{dt} = V \tag{5.18}$$

The equations (5.15 – 5.18) above are similar as the equations in the Level Flight. There is small change between the Level Flight. From equation (5.16), The Lift force is greater than Weight force acting on an aircraft. The altitude of an aircraft is increased by the result of this inequality. The vertical rate is dependent only upon the magnitude of Lift force. The magnitude of Lift force can be affected by factors, which have been listed in section 4.2.1. The main factor is a Lift to Drag Ratio (L/D ratio) (see section 4.2.1). There is written than L/D is affected by the angle of attack respectively by the pitch angle.

6. MODIFICATION AIRCRAFT MODEL

In this chapter, the implementation of aircraft model in MATLAB/SIMULINK has been outlined and compared with the theoretical knowledge from chapter 4. The main blocks and subsystems of this model have been described closely. Further, the modification of aircraft model by a time-varying mass parameter is defined according to the model of fuel consumption. In last part of this chapter, the model parameters are set up according to real aircraft Gulfstream G550.

6.1 AIRCRAFT MODEL IN SIMULINK

The implementation of nonlinear aircraft model is based on the model, which has been shown in the [1]. The individual blocks of this model had to be modified according to theoretical knowledge in chapter 4. The Figure 6.1 shows the implementation of nonlinear aircraft model in the MATLAB/SIMULINK. It´s based on the general block diagram in the Figure 4.1.

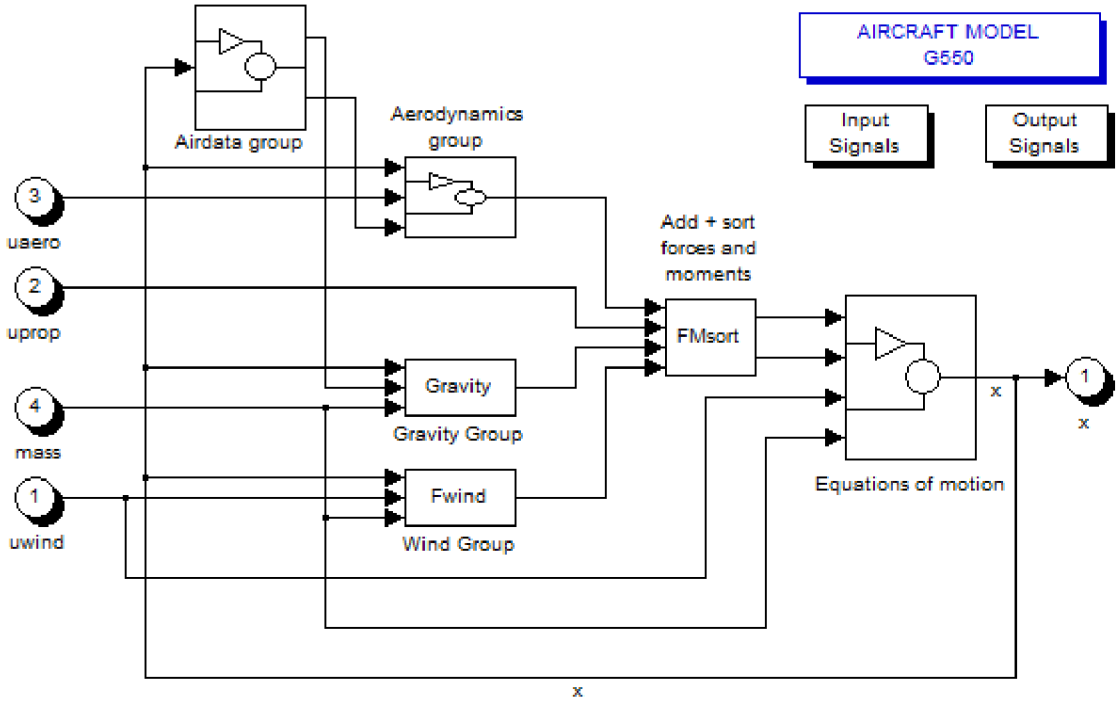

Figure 6.1: The MATLAB/SIMULINK implementation of the Aircraft Model

The input vectors of aircraft model are $\mathbf{u}_{aero}$, $\mathbf{u}_{prop}$, $\mathbf{u}_{wind}$ and mass which contain the deflection of elevator, thrust engine, wind components and aircraft weight. In this model, the wind forces are neglected. The last input of model is actual aircraft weight, which is changed every time by the model of fuel consumption (described hereafter). The output vector is state vector $\mathbf{x}$ which contain the airspeed, altitude and other (see section 2.4). There are any outputs, which can be defined in the aircraft model (e.g. temperature, Mach, Lift and Drag force, etc).

The Figure 6.2 shows the block of general aircraft model. The general aircraft model is masked subsystem with two vectors of parameters. The first is vector GM of geometrical data (see section 6.3.4) and second is initial state-space vector $\mathbf{x}_0$. There are summarized subsystems and blocks which have been shown in the Figure 6.1. This general aircraft model is used for CCC simulation (see chapter 8 and 9).

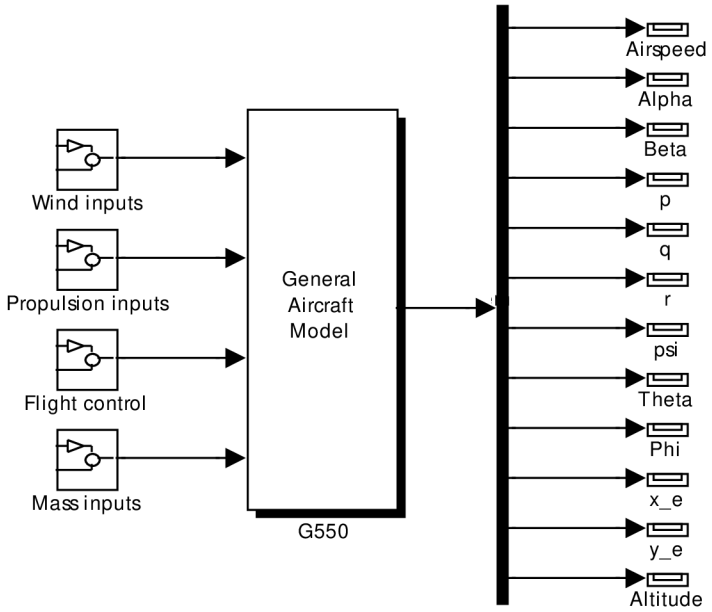

Figure 6.2: Block of the General Aircraft Model

6.1.1 Airdata Group

This subsystem computes airdata and atmospheric parameters (e.g. dynamic pressure and Mach number), which are required to determine the external forces and moments. The change of atmospheric parameters with change from troposphere to tropopause and vice versa is taken into account in this subsystem.

Subsystems

The subsystem Airdata Group includes these blocks:

- Atmosph: This block calls MATLAB function *GetAtmosphere* which computes atmospheric parameters (the ICAO Standard Atmosphere is used). The troposphere equations are used if altitude is less than 11 kilometer. Vice and versa the tropopause equations are used if altitude is higher than 11 kilometer.
- Airdata: This block computes the base variables (e.g. Mach number) which are always required to solve the equations of motion.

The equations used by these blocks have been discussed in section 4.3.

Input/Output parameters

There are table of block input and output parameters:

Type	Parameters	Description
Inputs	$\mathbf{x} = [V \ \alpha \ \beta \ p \ q \ r \ \psi \ \theta \ \varphi \ x_e \ y_e \ H]^T$	state vector
Outputs	$\mathbf{y}_{atm} = [\rho \ p_s \ T \ \mu \ g]^T$	basic atmospheric variables
	$\mathbf{y}_{ad} = [a \ M \ q_{dyn}]^T$	basic airdata variables

Table 6.1: Input/output parameters for the Airdata Group

6.1.2 Aerodynamics Group

This subsystem computes the contributions to the aerodynamic forces and moment upon the aircraft. There is used aerodynamic model from section 4.2.1. Only the vertical forces and moment contributions are considered. The specific calculation of lift, drag and pitching moment are defined in this model. Therefore the aerodynamic model is valid for this application only.

Subsystems

The subsystem Aerodynamics Group includes these blocks:

- Aeromod: This block computes dimensionless lift, drag and pitching moment coefficient for the aircraft.
- Dimless: This block computes dimensionless angular velocities.
- FMdims: This block converts the dimensionless force and moment coefficients to dimensional forces and moment.

The equations used by these blocks have been discussed in section 4.2.1.

Input/Output parameters

There are table of block input and output parameters:

Type	Parameters	Description
Inputs	$\mathbf{x} = [V \ \alpha \ \beta \ p \ q \ r \ \psi \ \theta \ \varphi \ x_e \ y_e \ H]^T$	state vector
	$\mathbf{u}_{aero} = [\delta_e \ \delta_a \ \delta_r \ \delta_f]^T$	control deflection
	$\mathbf{y}_{ad} = [a \ M \ q_{dyn}]^T$	basic airdata variables
Outputs	$\mathbf{y}_{dl} = \left[\frac{pb}{2V} \ \frac{q\bar{c}}{2V} \ \frac{rb}{2V}\right]^T$	dimensionless angular velocities
	$\mathbf{C}_{aero} = [C_D \ 0 \ C_L \ 0 \ C_M \ 0]^T$	aerodynamic coefficients
	$\mathbf{FM}_{aero} = [F_{X\,a} \ F_{Y\,a} \ F_{Z\,a} \ L_a \ M_a \ N_a]^T$	dimensional aerodynamic forces and moments

Table 6.2: Input/output parameters for the Aerodynamics Group

6.1.3 Gravity Group

This block computes the contributions to gravitational forces upon the aircraft. The equations which are used by this block have been discussed in section 4.2.3. The pitch and roll angle are needed to determine gravitational force (see equation 4.24). The variable gravitational acceleration with altitude is considered. These gravitational forces depend on the actual weight of aircraft. Therefore the actual weight of aircraft is input in to this block. The contributions of gravity forces are valid for any aircraft.

Input/Output parameters

There are table of block input and output parameters:

Type	Parameters	Description
Inputs	$\mathbf{x} = [V \ \alpha \ \beta \ p \ q \ r \ \psi \ \theta \ \varphi \ x_e \ y_e \ H]^T$	state vector
	$\mathbf{y}_{atm} = [\rho \ p_s \ T \ \mu \ g]^T$	basic atmospheric variables
	$\mathbf{m} = [mass]^T$	actual mass
Outputs	$\mathbf{F}_{grav} = [F_{X\,gr} \ F_{Y\,gr} \ F_{Z\,gr}]^T$	gravity force components

Table 6.3: Input/output parameters for the Gravity Group

6.1.4 Wind Group

This block computes the contributions to the wind forces upon the aircraft. The wind forces need to be added to the forces along the aircraft's body-axes when considering flight in nonsteady atmosphere. The equations of wind forces are depended on the wind velocity, the wind acceleration, and the roll, pitch, and yaw rates of the aircraft. The contributions of wind forces are valid for any aircraft. The equations used by these blocks have been discussed in section 4.2.4.

Input/Output parameters

There are table of block input and output parameters:

Type	Parameters	Description
Inputs	$\mathbf{x} = [V \ \alpha \ \beta \ p \ q \ r \ \psi \ \theta \ \varphi \ x_e \ y_e \ H]^T$	state vector
	$\mathbf{u}_{wind} = [u_w \ v_w \ w_w \ \dot{u}_w \ \dot{v}_w \ \dot{w}_w]^T$	components of wind velocity and acceleration
	$\mathbf{m} = [mass]^T$	actual mass
Outputs	$\mathbf{F}_{wind} = [F_{X\,w} \ F_{Y\,w} \ F_{Z\,w}]^T$	wind force components

Table 6.4: Input/output parameters for the Wind Group

6.1.5 FMsort

This block computes the components of the resulting forces and moment, and it stores the results in a separate force vector and moment vector. This aircraft model takes into account aerodynamic forces and moment, propulsive force, gravitational forces, and wind force. The equations used by these blocks have been discussed in section 4.2 (see equations 4.8 and 4.7).

Input/Output parameters

There are table of block input and output parameters:

Type	Parameters	Description
Inputs	$\mathbf{FM}_{aero} = \begin{bmatrix} F_{X\,a} & F_{Y\,a} & F_{Z\,a} & L_a & M_a & N_a \end{bmatrix}^T$	aerodynamic forces and moments
	$\mathbf{u}_{prop} = \begin{bmatrix} F_{X\,p} & F_{Y\,p} & F_{Z\,p} & L_p & M_p & N_p \end{bmatrix}^T$	propulsive forces and moments
	$\mathbf{F}_{grav} = \begin{bmatrix} F_{X\,gr} & F_{Y\,gr} & F_{Z\,gr} \end{bmatrix}^T$	gravity forces
	$\mathbf{F}_{wind} = \begin{bmatrix} F_{X\,w} & F_{Y\,w} & F_{Z\,w} \end{bmatrix}^T$	wind forces
Outputs	$\mathbf{F}_{tot} = \begin{bmatrix} F_x & F_y & F_z \end{bmatrix}^T$	total external forces
	$\mathbf{M}_{tot} = \begin{bmatrix} L & M & N \end{bmatrix}^T$	total external moments

Table 6.5: Input/output parameters for the FMsort

6.1.6 Equations of Motion

This subsystem computes the time-derivative of the state vector according to the state equations of motion (see section 2.4). This vector goes through an integrator block. The state vector of aircraft model is defined by this integrator.

Subsystems

The subsystem Equations of motion includes these blocks:

- uvw: This block computes the velocity components according to equations (2.13).
- 12 ODEs: This block computes the state equations, which have been discussed in section 2.4.

Input/Output parameters

There are table of block input and output parameters:

Type	Parameters	Description
Inputs	$\mathbf{F}_{tot} = \begin{bmatrix} F_x & F_y & F_z \end{bmatrix}^T$	total external forces
	$\mathbf{M}_{tot} = \begin{bmatrix} L & M & N \end{bmatrix}^T$	total external moments
	$\mathbf{u}_{wind} = \begin{bmatrix} u_w & v_w & w_w & \dot{u}_w & \dot{v}_w & \dot{w}_w \end{bmatrix}^T$	components of wind velocity and acceleration
	$\mathbf{m} = \begin{bmatrix} m \end{bmatrix}^T$	actual mass
Outputs	$\mathbf{x} = \begin{bmatrix} V & \alpha & \beta & p & q & r & \psi & \theta & \varphi & x_e & y_e & H \end{bmatrix}^T$	state vector

Table 6.6: Input/output parameters for the Equations of Motion

6.2 MODEL OF FUEL CONSUMPTION

In this chapter, the model of fuel consumption has been described. There before, the aircraft model in MATLAB/SIMULINK has been discussed (see section 6.1). The external forces and moments are depended directly on time (the fuel-burn decreases the weight of the airplane in time). The propulsive force (thrust) is directly input into the aircraft model. There are these requirements. The generation of thrust and change the weight of aircraft with time has to be ensured. These requirements can be achieved by the model of fuel consumption.

The model of fuel consumption is defined by block of Turbofan Engine System, which simulates the fuel consumption and generating thrust. The Turbofan Engine System is able to model any turbofan engine if the parameters are set up correctly. The parameters of Turbofan Engine System are set up according to the engine BR710, which is used in the Gulfstream G550. The table of these parameters is shown in the next section 6.3.

The Figure 6.3 shows model of fuel consumption. The thrust and fuel flow are generated upon the inputs and parameters of Turbofan Engine System. The Table 6.7 shows input/output vector of Turbofan Engine System. The value of thrust and fuel flow can be defined in metric or English unit. The model of fuel consumption is connected with dynamics in the aircraft model.

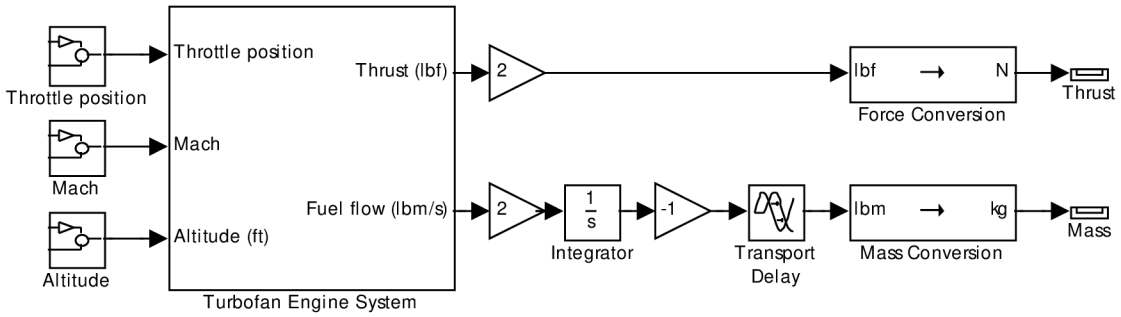

Figure 6.3: The Model of Fuel Consumption

Type	Parameters
Inputs	$\mathbf{u}_{en} = [Trottle\ M\ H]^T$
Outputs	$\mathbf{y}_{en} = [T\ \ FF]^T$

Table 6.7: Input/output parameters of the Model of Fuel Consumption

The model of fuel consumption generates directly thrust and actual value of fuel consumption. But the change of aircraft weight is needed for the aircraft model. The conversion between fuel flow and change of aircraft weight is defined by integrator (see Figure 6.3). In each step of simulation, the actual fuel flow is subtracted from initial state (weight of aircraft). At the end model of fuel consumption is mass conversion from pound-mass to kilogram, because the aircraft model is defined in the metric units.

6.3 SET UP MODEL PARAMETERS

This chapter provides the general data for the Gulfstream G550. The aircraft model is set up according to these aircraft. Next, the setting individual components from the aircraft model have been described.

6.3.1 General Data of Gulfstream G550

The Gulfstream G550 was selected as a real aircraft for setting aircraft model. There is basic information about the Gulfstream G550.

The picture of the aircraft has been shown in Figure 6.4. The Gulfstream G550 is long range business jet aircraft. The Gulfstream G550 is powered by two BMW / Rolls Royce BR710C4-11 high bypass ratio turbofan engines. The Gulfstream G550 has a range of 12 501 km at Mach 0.80 and a high-speed cruise capability of Mach 0.87. The maximum operating altitude is 51,000 ft. The Table 6.8 and Table 6.9 show general engine and aircraft data of Gulfstream G550. [11]

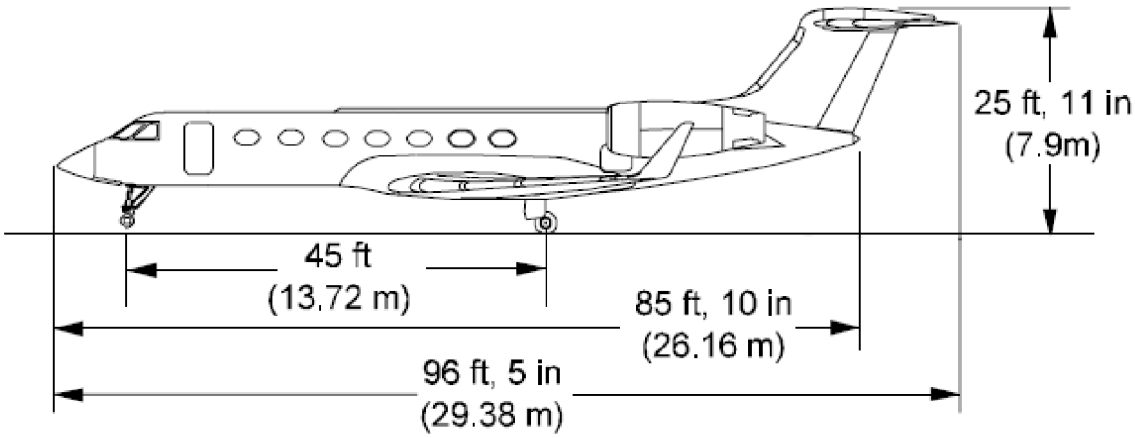

Figure 6.4: The Gulfstream G550 [12]

Engine	Two Rolls-Royce BR710 C4-11
Rated Takeoff Thrust	15 385 lb / 68.4 kN
Thrust specific fuel consumption	0.39
Maximum sea-level static thrust	14 750 lb / 62.3 kN

Table 6.8: The general engine data of the Gulfstream G550 [11]

Manufacturer	General Dynamic´s Gulfstream
Type of aircraft	Business jet
Wing span b	93.6 ft / 28.50 m
Wing area S	1 137 ft^2 / 105.6 m^2
Mean aerodynamic chord c	13.86 ft / 4.23 m
Overall Length	96.5 ft / 29.39 m
Overall Height	25.1 ft /7.87 m
Maximum Takeoff Weight	91000 lb / 41277 kg
Maximum Landing Weight	73300 lb / 34 156 kg
Maximum Zero Fuel Weight	54 500 lb / 24 721 kg
Maximum Fuel Weight	41 300 lb / 18 733 kg
Maximum Range	6750nm / 12501 km
Normal Cruise	Mach 0.80 / 459ktas / 850km/h
High Speed Cruise	Mach 0.87 / 500ktas / 926km/h
Takeoff Distance	5910 ft / 1801 m
Landing Distance	2770 ft / 844 m
Initial Cruise Altitude	41000 ft / 1249 m
Maximum Cruise Altitude	51000ft / 15545 m

Table 6.9: The general aircraft data of the Gulfstream G550 [11]

6.3.2 Set up the Aerodynamic Model

The aerodynamic model is the most important part of the aircraft model. The aircraft dynamic are defined by this aerodynamic model (see section 4.2.1). In this chapter, the parameters of aerodynamic model are set up. The parameters are adjusted in part according to [14] and partly experimentally to match the Gulfstream G550.

The aerodynamic model is computed in the block Aeromod. There are the aerodynamic equations from in section 4.2.1. The coefficients of these equations are implemented directly in the equations. These coefficients are necessary to calculate the aerodynamic forces and moment acting on the aircraft (lift, drag, and pitching moment).

These coefficients are listed in the Table 6.10.

Lift coefficients	$C_{L_0} = 0.276$ $C_{L\alpha} = 0.095$
Drag coefficients	$C_{D_0} = 0.01491$ $AR = 7.36$ $e = 0.95$
Pitching moment coefficients	$C_{m\alpha} = -0.2$ $C_{mq} = -1$ $C_{m\delta_e} = -3.9$

Table 6.10: The coefficients of the aerodynamic model

6.3.3 Set up the Model of Fuel Consumption

The main part model of fuel consumption is the block Turbofan Engine System (see section 6.2). This block is masked subsystem with five parameters. These parameters are shown in Table 6.11.

Some parameters were set up according to the general data listed above. The others are set up to match the engine BR710 (e.g. the parameter ratio of installed thrust it uninstalled thrust was set up experimentally).

Some information about the Turbofan Engine System is listed in the [15].

Initial Thrust	2184.5	[lb]
Maximum sea-level static thrust	16000	[lb]
Fastest engine time constant at sea-level static	0.005	[s]
Sea-level static thrust specific fuel consumption	0.39	[-]
Ratio of installed thrust to uninstalled thrust	1.2	[-]

Table 6.11: The parameters of the Turbofan Engine System

6.3.4 Set up the Geometrical Data

These data are used for computing equations, which have been described in chapter 2 and 4. The geometrical data are inserted in the vector GM, which contains the moments and products of inertia, mean aerodynamic chord, wing span, and wing area. The numerical values of GM have been shown in Table 6.12.

$[\bar{c}$	b	S	I_{xx}	I_{yy}	I_{zz}	J_{xy}	J_{xz}	$J_{yz}]$
[4.23	28.5	105.6	5992	21687	25779	0	1604	0]

Table 6.12: The geometrical data of the vector GM

7. LINEARIZATION AIRCRAFT MODEL

This chapter deals with the linearization of the aircraft model above. There are discussed problems with linearization of the aircraft model. Next, the reasons for linearization of model aircraft have been written. In the chapter 3, the theoretical background about linearization system via Taylor series is described. This method is commonly used for linearization.

7.1 OVERVIEW

According to task, the theoretical linearization has been acquainted (see charter 3). With this background, the state regulator has been tried design with the aim to optimize vertical flight profile.

The aircraft model is nonlinear. For application the classical linear control theory the linear aircraft model is needed.

There are some problems, which have to be discussed. The higher order terms are not considered around the operating point. Some information about system can be lost by this assumption. The nonlinear function is replaced by a straight line at a given operating point. Therefore, there are lost information about the further course of the original curve. The replacement is valid only near the operating point (how "near" depends on how nonlinear the function is). This problem can be better explained by the following Figure 7.1.

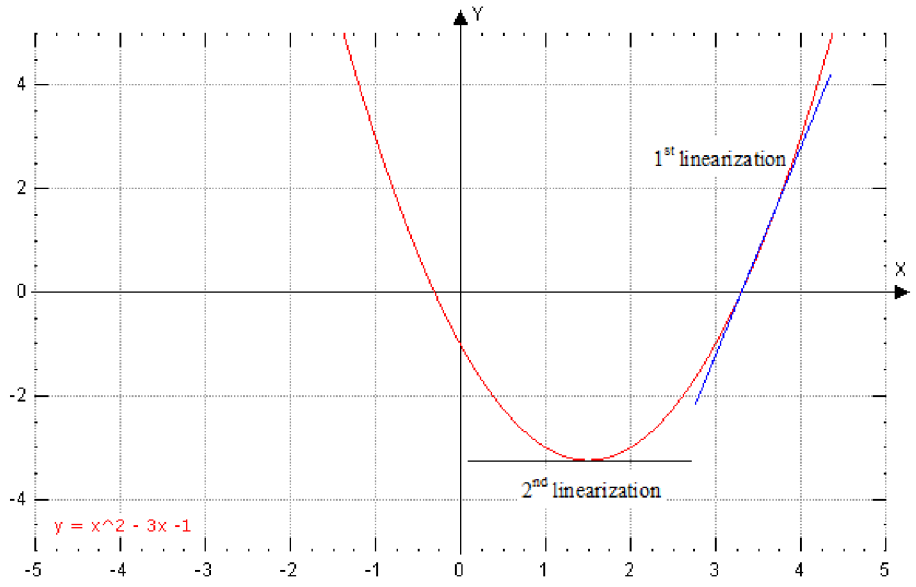

Figure 7.1: Examples of the linearization

The Figure 7.1 shows two types of linearization around the different operating point. The accuracy of linearization is depended on the choice of operating point. While the first linearization is correct, because the nonlinear function is followed by the straight line of linearization. The second linearization is completely wrong, because

there is the maximum of nonlinear function. The small different from operating point, the nonlinear function is not followed by the straight line of linearization.

There is another problem, which has to be considered. It is the complexity of the nonlinear system. The linear system is given by the partial derivatives of the nonlinear system around the operating point. If the nonlinear system is very complicated, then the partial derivatives cannot be obtained.

For linearization the aircraft model, the operating point is needed. There is discussed the operating point. The operating point is defined by the state vector $\mathbf{x}$. The Continuous Climbing Cruise is simulated with maximum Lift to Drag ratio (see chapter 5 and 8). The Figure 7.2 shows graphical function of the L/D ratio to angle of attack. If the L/D_{max} is considered the linear system is not achieved for this operating point.

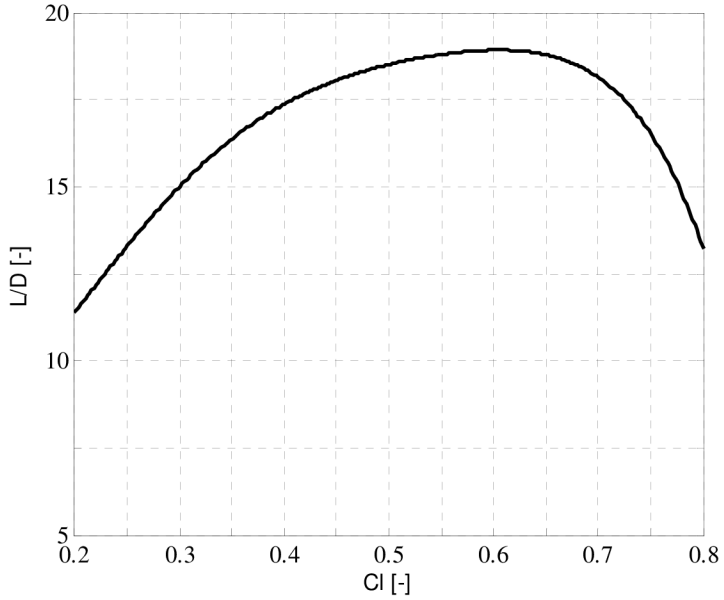

Figure 7.2: L/D polar of the Gulfstream G550: M = 0.77; H = 460FL [14]

The operating point is unfitting for the linearization. The nonlinear system is too complicated for linearization. To use the partial derivative, the nonlinear state equations have to be expressed only with state variables, inputs, outputs, and constants. For example, the complexity of the nonlinear system is shown in the equations below. There is equation of true airspeed, before the partial derivatives.

$$\dot{V} = \frac{1}{m}(F_x \cos\alpha\cos\beta + F_y \sin\beta + F_z \sin\alpha\cos\beta) \qquad (7.1)$$

where

$$F_x = F_{X\,a} + F_{X\,p} + F_{X\,gr} + F_{X\,w}; \qquad F_y = 0; \qquad F_z = F_{Z\,a} + F_{Z\,gr} + F_{Z\,w}$$

where

$$\begin{matrix} F_{X\,a} = L\sin\alpha - D\cos\alpha \\ F_{Z\,a} = -L\cos\alpha - D\sin\alpha \end{matrix}; \qquad F_{X\,p} = T; \qquad \begin{matrix} F_{X\,gr} = -mg\cdot\sin\theta \\ F_{Z\,gr} = mg\cdot\cos\theta\cos\varphi \end{matrix}; \qquad \begin{matrix} F_{X\,w} = 0 \\ F_{Z\,w} = 0 \end{matrix}$$

where

$$L = \frac{1}{2} C_L \rho V^2 S; \qquad D = \frac{1}{2} C_D \rho V^2 S$$

where

$$C_L = C_{L_0} + C_{L_\alpha} \alpha; \qquad C_D = C_{D_0} + \frac{\left(C_{L_0} + C_{L_\alpha} \alpha\right)^2}{\pi \cdot AR \cdot e}$$

Substituting these relations into the equation (7.1), the state equation only with state variables, inputs, outputs, and constants is given.

$$\dot{V} = \frac{1}{m}\left[\left(\frac{1}{2}\left(C_{L_0} + C_{L_\alpha}\alpha\right)\rho V^2 S\right)\sin\alpha - \left(\frac{1}{2}\left(C_{D_0} + \frac{\left(C_{L_0} + C_{L_\alpha}\alpha\right)^2}{\pi \cdot AR \cdot e}\right)\rho V^2 S\right)\cos\alpha + T - mg \cdot \sin\theta\right] \cdot$$
$$\cdot \cos\alpha\cos\beta +$$
$$+\frac{1}{m}\left[-\left(\frac{1}{2}\left(C_{L_0} + C_{L_\alpha}\alpha\right)\rho V^2 S\right)\cos\alpha - \left(\frac{1}{2}\left(C_{D_0} + \frac{\left(C_{L_0} + C_{L_\alpha}\alpha\right)^2}{\pi \cdot AR \cdot e}\right)\rho V^2 S\right)\sin\alpha + mg \cdot \cos\theta\cos\varphi\right] \cdot$$
$$\cdot \sin\alpha\cos\beta$$

From this equation, there is shown the nonlinear functions (as sin, cos, multiplication, square, etc.) of the state variables. These functions cannot be replaced by the straight line for operating point above.

7.1.1 Summary

From aircraft model, which has been defined above, the linear aircraft model cannot be achieved by the linearization via Taylor series. The reasons are discussed above.

Consequently, the state controller cannot be proposed. This deficiency was completely solved by the classical controllers (PI regulators) and optimization via Matlab Optimization Toolbox. The results are listed below.

8. SIMULATION OF CONTINUOUS CLIMBING CRUISE

In this part of thesis have been described results of the simulation Continuous Climbing Cruise (CCC). Firstly, the control of the aircraft model is proposed for simulation the vertical flight profile. There are set initial values of the aircraft model parameters for the simulation CCC. Next, the important characteristics of state vector (such as altitude and airspeed) are shown in the section 8.2. In the last part, an analysis of results is discussed and the results are compared with CCC from X-Plane simulation.

8.1 OVERVIEW

For simulation the CCC knowledge about the CCC is needed. Currently, there are three climb techniques used in the cruise phase (see Figure 8.1). In the chapter 5, these techniques have been discussed. There is written, that the cruise climb optimizes the vertical profile with respect to fuel consumption. This claim can be verified by the simulation of CCC. The optimal vertical flight profile is considered with respect of fuel consumption to distance.

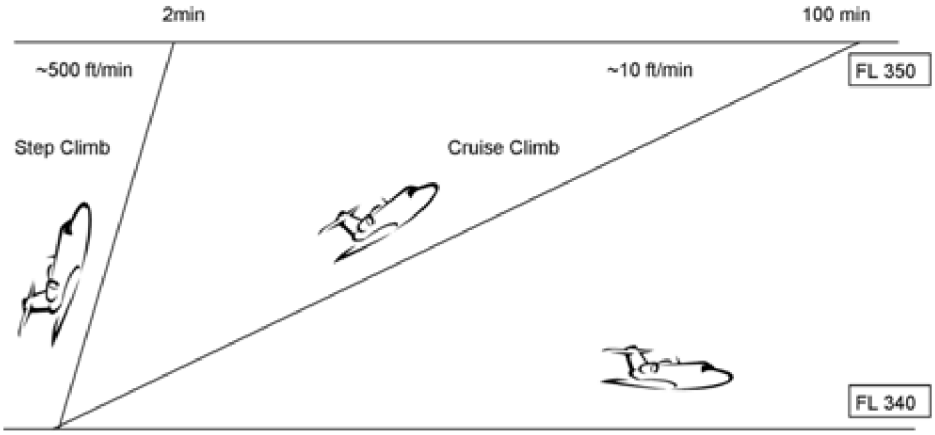

Figure 8.1: Difference between Level Flight, Step Climb and Cruise Climb

In the aircraft, the requirement on the control system always establishes efficient cruise altitude. The efficient cruise altitude is the function of weight of aircraft, temperature, wind speed and other specific conditions.

In the level flight, the same barometric altitude is held throughout the flight. The aircraft fly on the altitude that provides the most efficient cruise at the start of flight. But the efficient altitude is not same at the start and at the end of the flight. The efficient altitude is increased with decrease the weight of aircraft. The level flight technique is not optimal from fuel consumption perspective.

During a step climb, the efficient altitude is achieved throughout the flight. But a lot of fuel is burned by the change from one cruise altitude to another. Also the great

drag has to be overcame during maneuver. The step climb technique is not also optimal with respect of fuel consumption, but it is more efficient technique than the level flight.

The last type of flight, which has been discussed in the chapter 5, is cruise climb. It is Continuous Climbing Cruise. A cruise altitude is gradually increased from initial cruise altitude to a final cruise altitude. The optimal vertical flight profile with respect fuel consumption can be ensured by this fly. In the section 5.3, there is written how can be the continuous climbing cruise achieved.

In the section 8.1.1 the proposal of the pitch angle and Mach number controller for simulation the CCC is described. In the section 8.1.2 the parameters for CCC simulation are listed.

8.1.1 Pitch angle and Mach number Controller

In this section, the proposal of longitudinal Auto Pilot (A/P) and Auto Thrust (A/THR) is discussed. The aircraft model, which has been shown above, is controlled by these controllers. In order to simulate the CCC these controllers are needed.

For the following proposal of longitudinal Auto Pilot and Auto Thrust, basic knowledge about the flight systems in an aircraft is needed. Therefore the flight systems are described. This brief background can help to reader understand proposal of controllers and a consequently CCC simulation. The proposed controllers are not complete Auto Pilot and Auto Thrust, which can be found in the Gulfstream G550. The controllers cannot be used same as the (A/P) and (A/THR), but completely comply with our application.

Avionics system called the Flight Management & Guidance System (FMGS) is standard equipment in the Gulfstream G550. That system assists the pilot with flight planning and automatically controlling the aircraft. The FMGS provide Flight Management (FM) and Flight Guidance (FG) functions. It reduces cockpit workload, improves efficiency and eliminates many routine operations generally performed by the pilots. [5]

The main FM functions are: [5]

- Navigation
- Flight planning
- Performance prediction and optimization
- Provision of information to cockpit display (MDCU, ND, PFD)

The main FG functions are: [5]

- Flight Direction (FD)
- Auto Pilot (A/P)
- Auto thrust (A/THR)

From these definitions, the flight trajectory and performance throughout the flight is computed by the control law in the flight management. The flight trajectory and performance is computed according to Flight Plan, which contains a lot of data (e.g. strategic data as CI, CRZ FL, ZFCG, tactical data as TOC, TOD, SPD LIMIT, etc.).

The some optimization criterion or instructions from ATC are considered during flight planning. In-flight, the reference data (as altitude, vertical rate, airspeed, etc.) for an A/P and an A/THR are defined by the flight management. The control laws in the flight management are based upon advanced control theory. These systems are know-how of companies, which deal with flight control design. The reference data for simulation CCC are discussed in the next section 8.1.2. And the reference data for fuel optimal CCC are given in the chapter 9.

From the definitions above, an aircraft is controlled by the control law in the flight guidance. The reference data for an A/P and an A/THR are generated by the flight management or directly by a pilot. The automatic control of state variables in an aircraft is ensured by the flight guidance. For example; an automatic control of altitude or vertical rate. In the flight guidance, the control laws are based upon a classical control theory. The classic controllers (a PI and PID regulators) are considered as the control law in the A/P or an A/THR. The design of these controllers is simpler than the above controllers of flight management. There are requirements to control in real time and the maximum reliability. The proposal of longitudinal A/P and A/THR can be included in the flight guidance system.

Pitch Angle Controller

The similar controller has been discussed in the [19]. The Pitch Angle Controller (PAC) is used to control the pitch angle θ of aircraft model. The PAC has been set experimentally. This controller is the basic longitudinal A/P. It controls the pitch angle θ by applying appropriate deflections of the elevator if the actual pitch angle θ differs from the desired reference value. There is applied a PI controller in order to make sure that no steady-state errors in the pitch angle θ is remain. A feedback loop of the pitch rate (q) to the elevator has been included to compensate for the small decrease in damping of the short-period mode due to the θ-feedback. [19]

The MATLAB/SIMULINK implementation of the PAC is shown in Figure 8.2. The feedback signals are obtained from state vector **x** in the aircraft model. The integrator in the controller has to be limited in order to prevent *windup effect*. Without an *anti-windup limiter*, it can take a long time before the integrator is unloaded, which degrades the autopilot performance. [18] [19]

The maximum feasible deflection of the elevator δ_e and pitch angle θ is listed in the Table 8.1.

Signal	Lower boundary	Upper boundary
θ	1 [°]	5 [°]
δ_e	-13 [°]	24 [°]

Table 8.1: Bounds of the signal for the Gulfstream G550 [13]

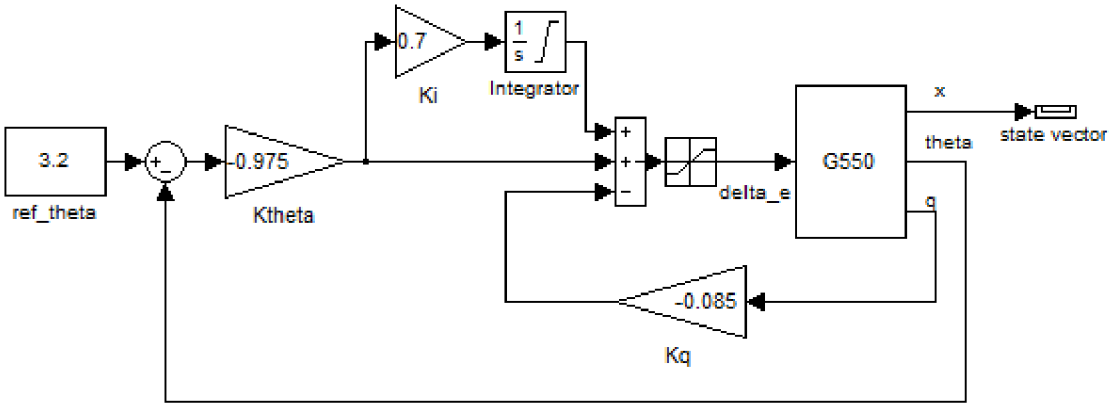

Figure 8.2: Block diagram of the Pitch angle controller in the SIMULINK

The output of the PI controller is deflections of the elevator $\delta_e(t)$. The PI algorithm is defined by the equation (8.1). The values of controller parameters are listed in the Table 8.2.

$$\delta_e(t) = K_\theta \left(e(t) + \frac{1}{T_i} \int_0^t e(t) \right) + K_q q(t) \qquad (8.1)$$

Parameter	Value
K_θ	-0.975
K_q	-0.085
Ti	1.43 s

Table 8.2: The parameters of the Pitch angle controller

Mach number Controller

There is a similar controller as above. The Mach number Controller (MC) is used to control the Mach number M of the aircraft model. The MC has been set experimentally. This controller is the basic A/THR. It controls the Mach number M by applying appropriate throttle position if the actual Mach number M differs from the desired reference value. There is applied also a PI controller. [19]

The MATLAB/SIMULINK implementation of the MC is shown in Figure 8.7. The feedback signal is obtained from block Airdata in the subsystem Airdata Group (see section 6.1.1). There is applied an *anti-windup limiter* also. The maximum feasible throttle position is interval from zero to one.

The output of the PI controller is throttle position. The PI algorithm is defined by the equation (8.2). The values of controller parameters are listed in the Table 8.3.

$$u(t) = K \left(e(t) + \frac{1}{T_i} \int_0^t e(t) \right) \qquad (8.2)$$

Parameter	Value
K	1000
Ti	10 s

Table 8.3: The parameters of the Mach number controller

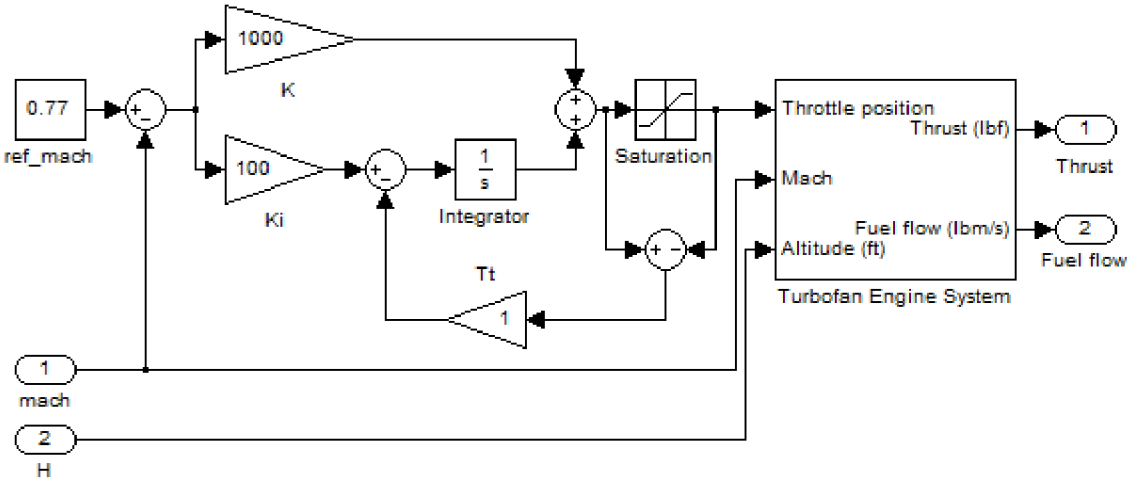

Figure 8.3: Block diagram of the Mach number controller in the SIMULINK

8.1.2 Set up parameters of the CCC Simulation

In this section, the parameters of CCC simulation have been discussed. There is the value of initial state vector, the time simulation, and definition of reference data for controllers. In order to simulate the CCC these parameters are needed.

The requirements of CCC simulation are listed in Table 8.4. All of these requirements are set according to supervisor recommendation.

Initial requirements	Parameter
Mass of aircraft	m = 36600 kg
Initial altitude	H = 460FL (14000 m)
Mach number	M = 0.77
Distance flown	x_e = 4000 km (2000 nm)
Lift to Drag ratio	L/D_{max}

Table 8.4: The requirements of the CCC simulation

The initial state vector $\mathbf{x}_0$, time simulation, and reference data for controllers are expressed from the requirements of CCC simulation. Some parameters of simulation are expressed directly from requirements (as initial altitude and mass of aircraft). Others have to be computed. The true airspeed is given from Mach number as $V = M \cdot a$. The simulation is not considered with respect the time. But there is considered distance

flown. Therefore, the simulation is stopped after the distance flown is equal to 2000 nm. The last requirement, the Lift to Drag Ratio upon the maximum has to be achieved. The L/D ratio diagram is dependent upon an aircraft, altitude and Mach number. The Figure 8.4 shows example of L/D polar for the Gulfstream G550.

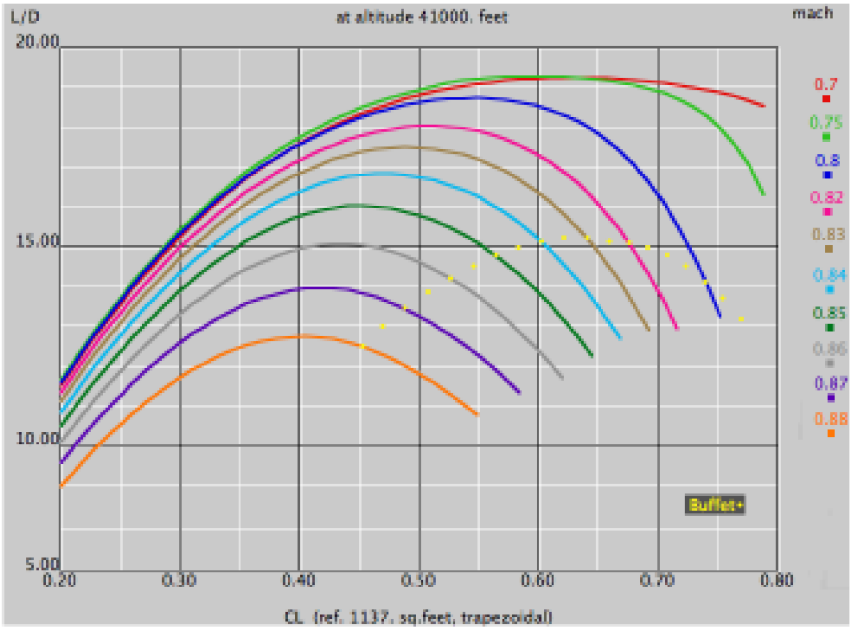

Figure 8.4: Example of the L/D polar [24]

The required L/D ratio can be achieved by the vertical rate and vice versa (see section 5.3). In the Table 8.5, there is listed the value of initial state vector for the CCC simulation. These data are used for setting the initial condition of subsystem Equations of Motion, which have been described in chapter 2. The initial data are inserted in the vector $\mathbf{x}_0$, which is second vector of parameters for masked subsystem G550. The initial state vector $\mathbf{x}_0$ is set according to requirements above.

Parameter	Value	Unit
V	227.21	$[m \cdot s^{-1}]$
α	3.2	[°]
β	0	[°]
p	0	$[° \cdot s^{-1}]$
q	0	$[° \cdot s^{-1}]$
r	0	$[° \cdot s^{-1}]$
φ	0	[°]
θ	3.2	[°]
ψ	0	[°]
x_e	0	[m]
y_e	0	[m]
H	460	[FL]

Table 8.5: The value of the initial State vector X_0

8.2 RESULTS OF SIMULATION

In this charter, the results of the CCC simulation are presented. The CCC simulation has been set according to the parameters above.

The following figures show the step response of controlled values in the regulation of the Pitch Angle Controller and the Mach number Controller. The actuating signals of both regulators are also shown.

From Figure 8.5, the desired value of theta is exactly tracked by the controlled value of theta. The transient performance is very short. The Pitch Angle Controller is proposed correctly. The state parameters are not affected by the transient performance of the pitch angle.

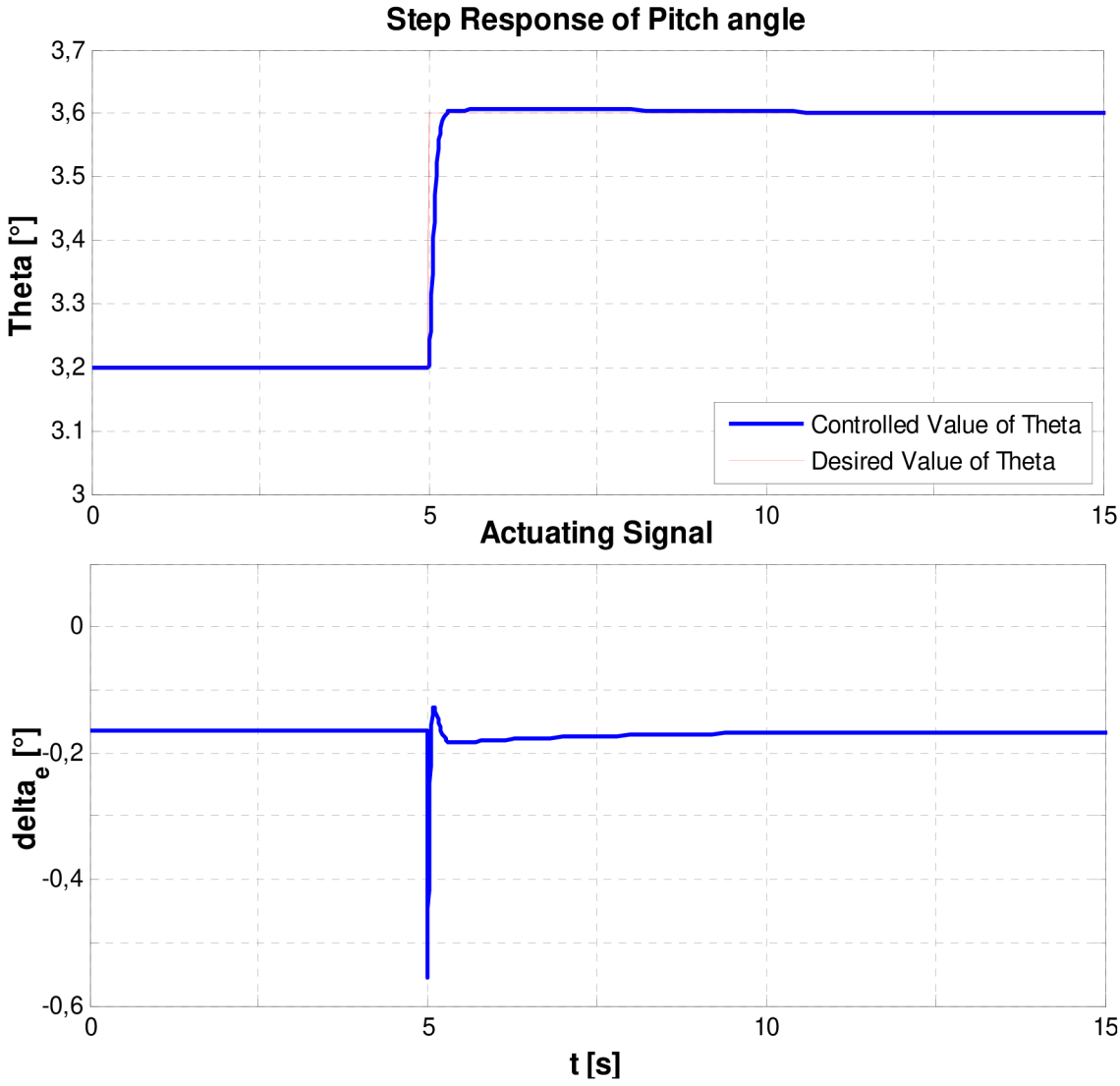

Figure 8.5: Step response of the Pitch angle and the acting signal of the PAC

Figure 8.6 shows the desired and controlled value of Mach number. There are first step response from M=0.77 to M=0.76. The transient performance is short. The controlled value of Mach number can be tracked by the Mach Controller. But for the second step response from M=0.76 to M=0.77, the controlled value of Mach number is

not tracked by the MC. The relative slow transient performance is caused by the saturation of the actuator (throttle). Despite this step response the Mach number Controller is proposed correctly. The state parameters are not affected by the transient performance of the Mach number.

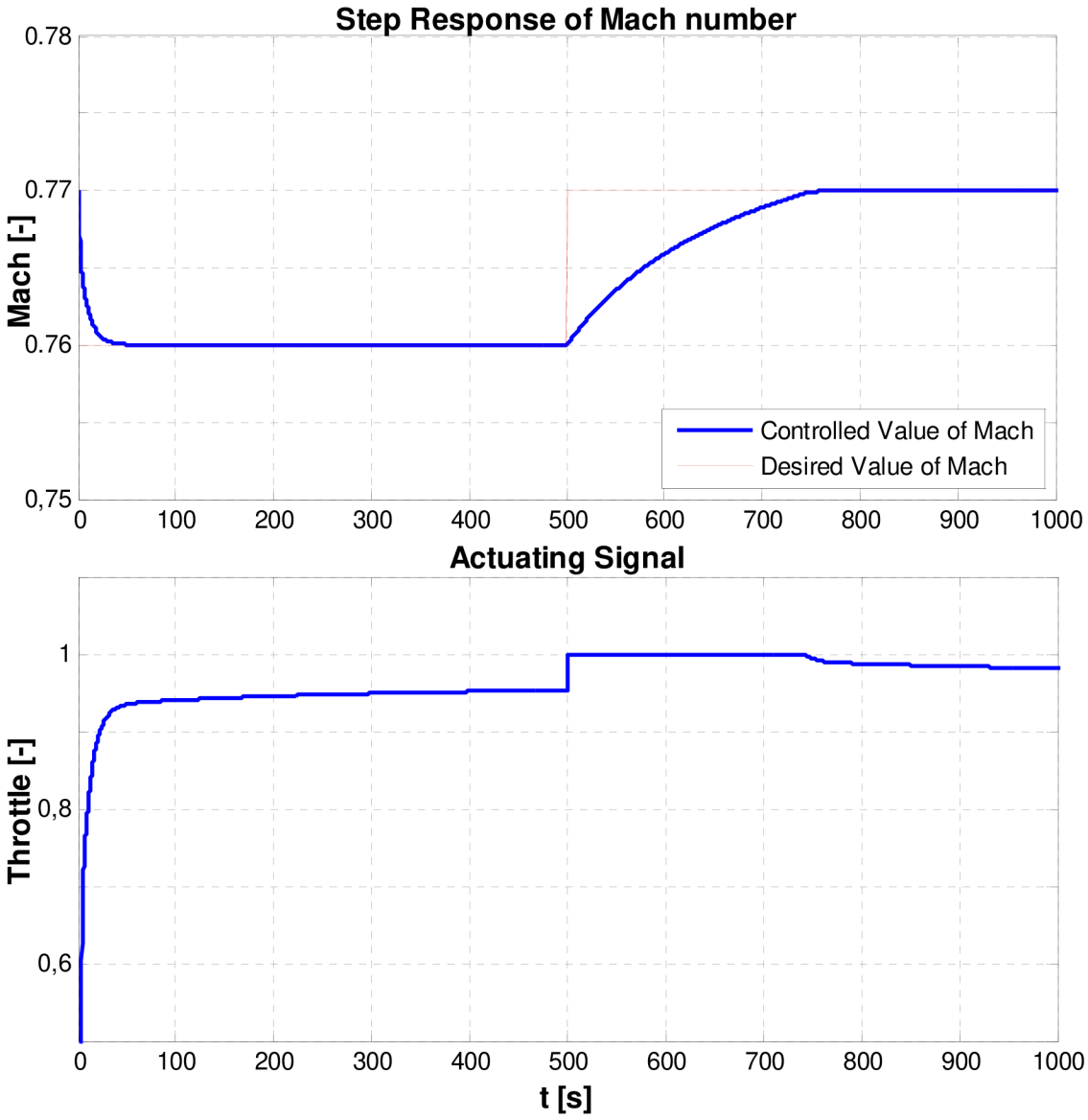

Figure 8.6: Step response of the Mach number and the actuating signal of the MC

The Figure 8.7 shows block-diagram in MATLAB/SIMULINK, which is used for CCC simulation. The SIMULINK schema is composed of the components, which have been described above. The general aircraft model (see section 6.1) is the main part of diagram. Another important part is the subsystem with Mach number Controller and the Model of Fuel Consumption. There is computed the thrust and actual mass of aircraft. In last part, the subsystem with Pitch angle Controller is implemented. From the block *Stop simulation after 4000km*, there is checked the distance flown. The simulation is stopped if the distance flown is equal to 4000km.

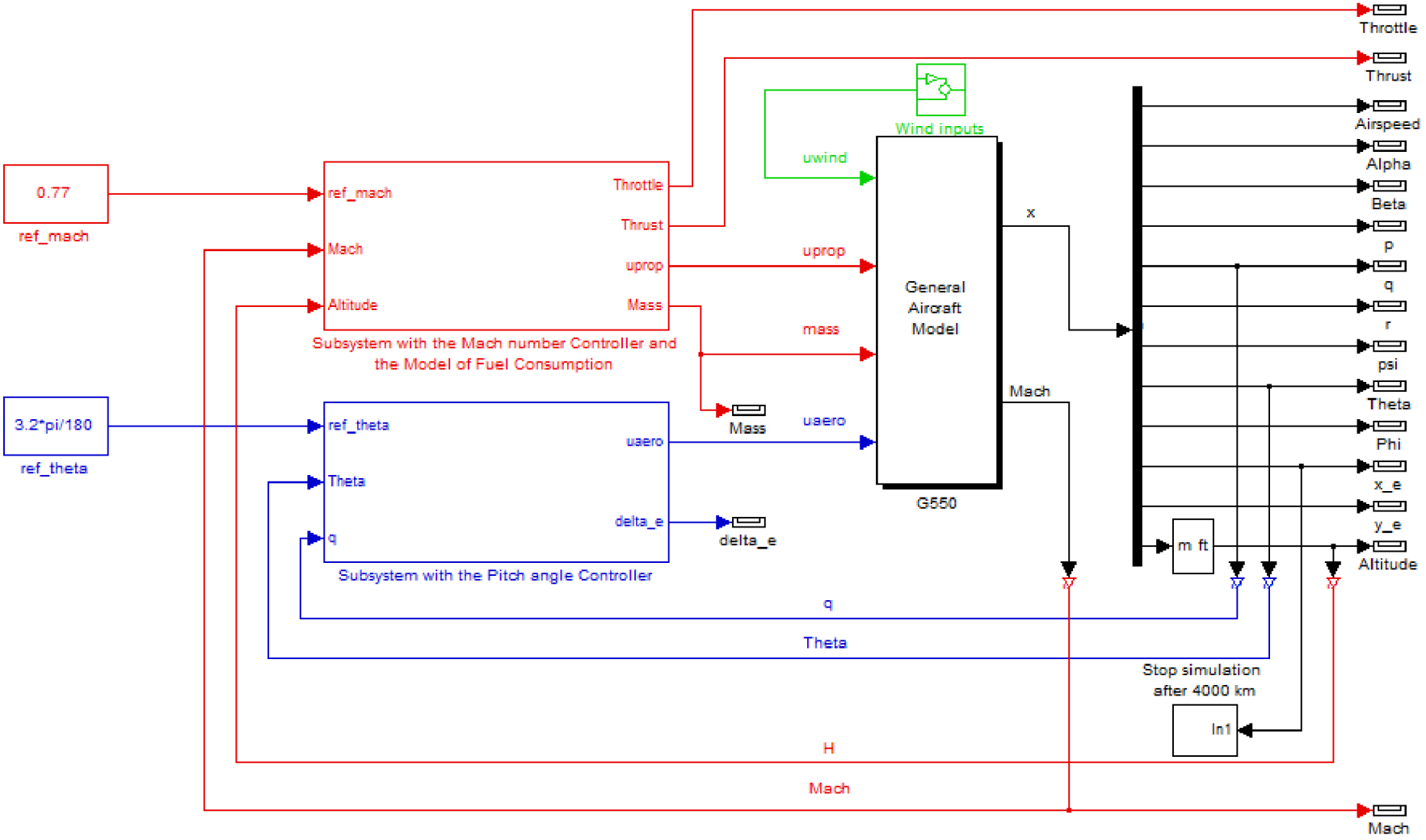

Figure 8.7: Block diagram for the CCC simulation

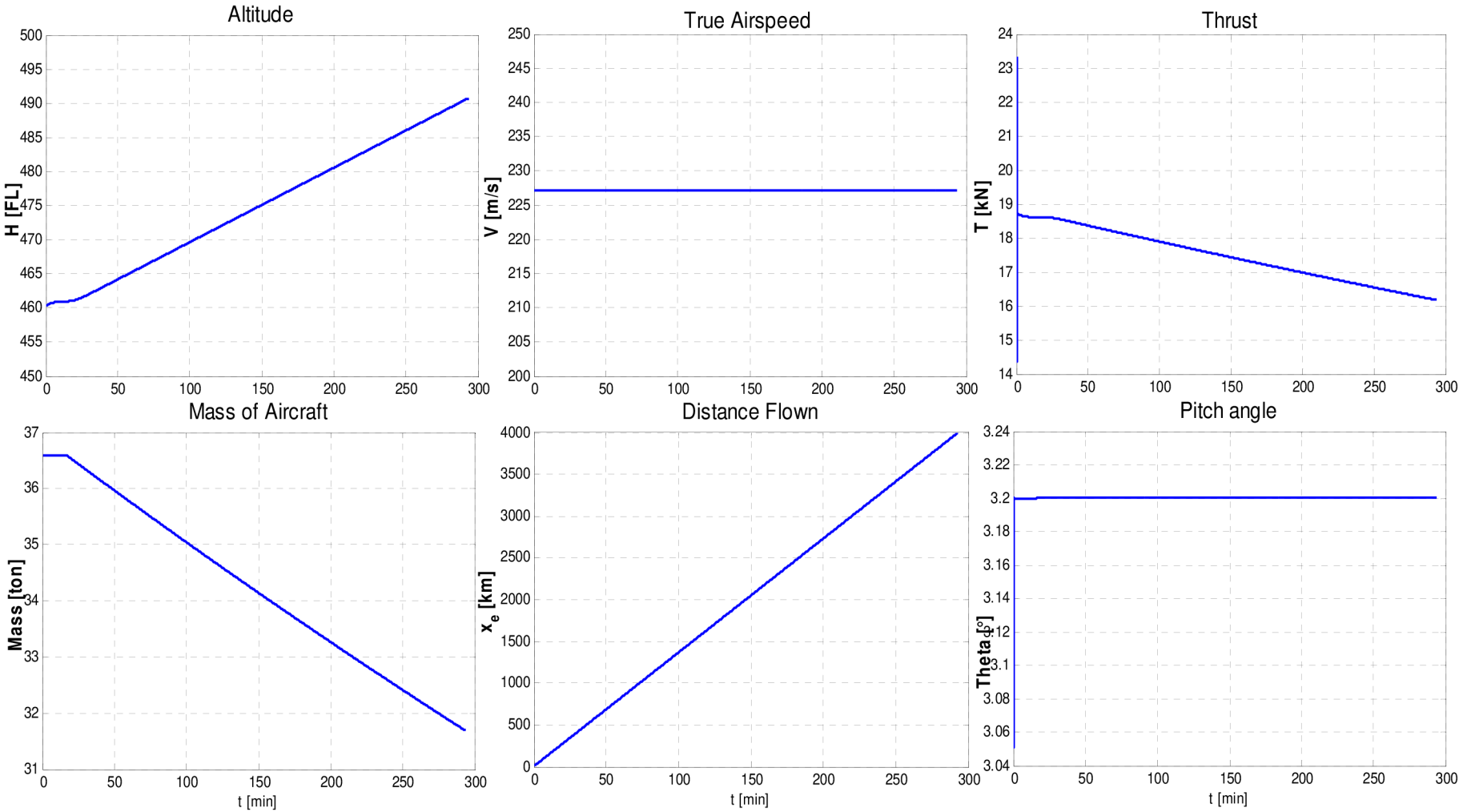

Figure 8.8: Graphical function of the state variables

The Figure 8.8 shows the graphical function of the important state variables for the CCC simulation. There are validated the theoretical assumptions, which have been listed above. The altitude increases linearly from launching the fuel consumption. The true airspeed and pitch angle are controlled upon the desired value. And finally, the desired distance flown is achieved.

8.3 DISCUSSION OF RESULTS

In this chapter, the main results of the CCC simulation are summarized. There are listed the fuel consumption per distance flown, vertical rate, matching theoretical L/D_{max} with simulated L/D_{max} and comparison the CCC simulation with the X-plane CCC simulation.

The one of the requirements, the L/D ratio has to be set upon the maximum value. This requirement is given from graphical function of L/D ratio (see Figure 8.9), there is reference L/D characteristic from the simulation program Piano [14] and the L/D characteristic, which is given from our simulation. During the CCC simulation, the value of L/D is held upon the maximum value.

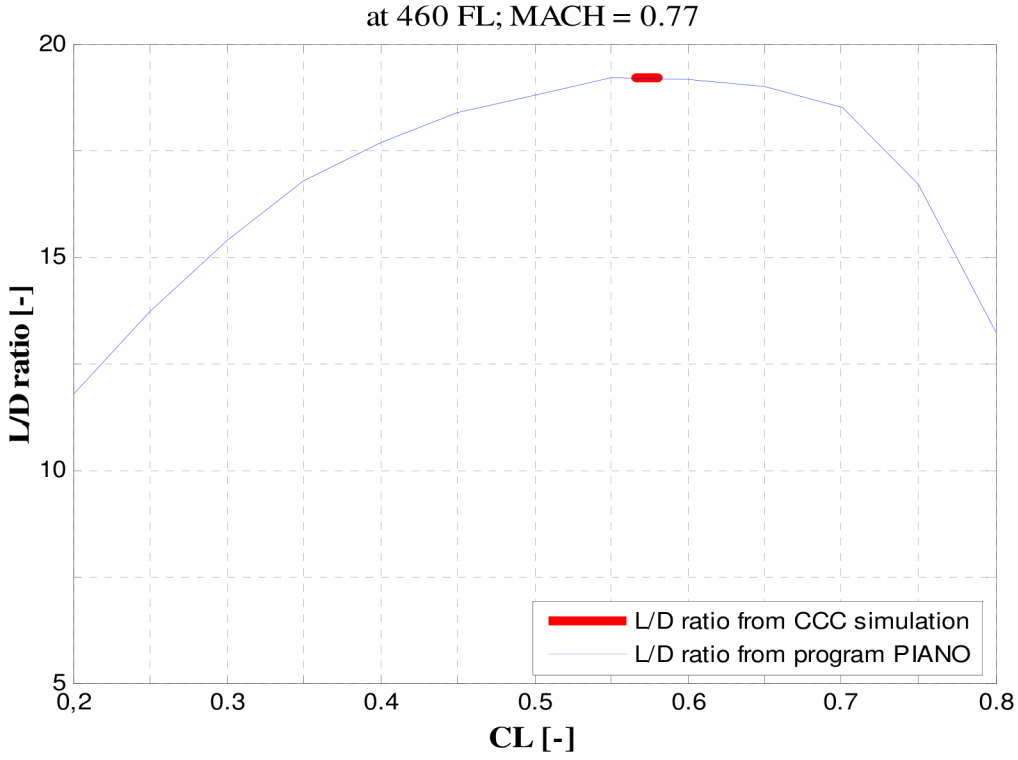

Figure 8.9: Graphical function of the L/D

The Figure 8.10 shows a comparison the CCC simulation with the X-plane CCC simulation. There is difference between our simulation and simulation from the X-plane. This difference is due to different lost of mass (see Figure 8.10).

The speed of climb per time is defined by the vertical rate. The vertical rate is given from graphical function of altitude (see Figure 8.10). From this Figure, the vertical rate is equal to slope of line. The slope of line is expressed in the unit Flight

Level per minutes. For expressed in the unit feet per minutes, the slope of line times hundred.

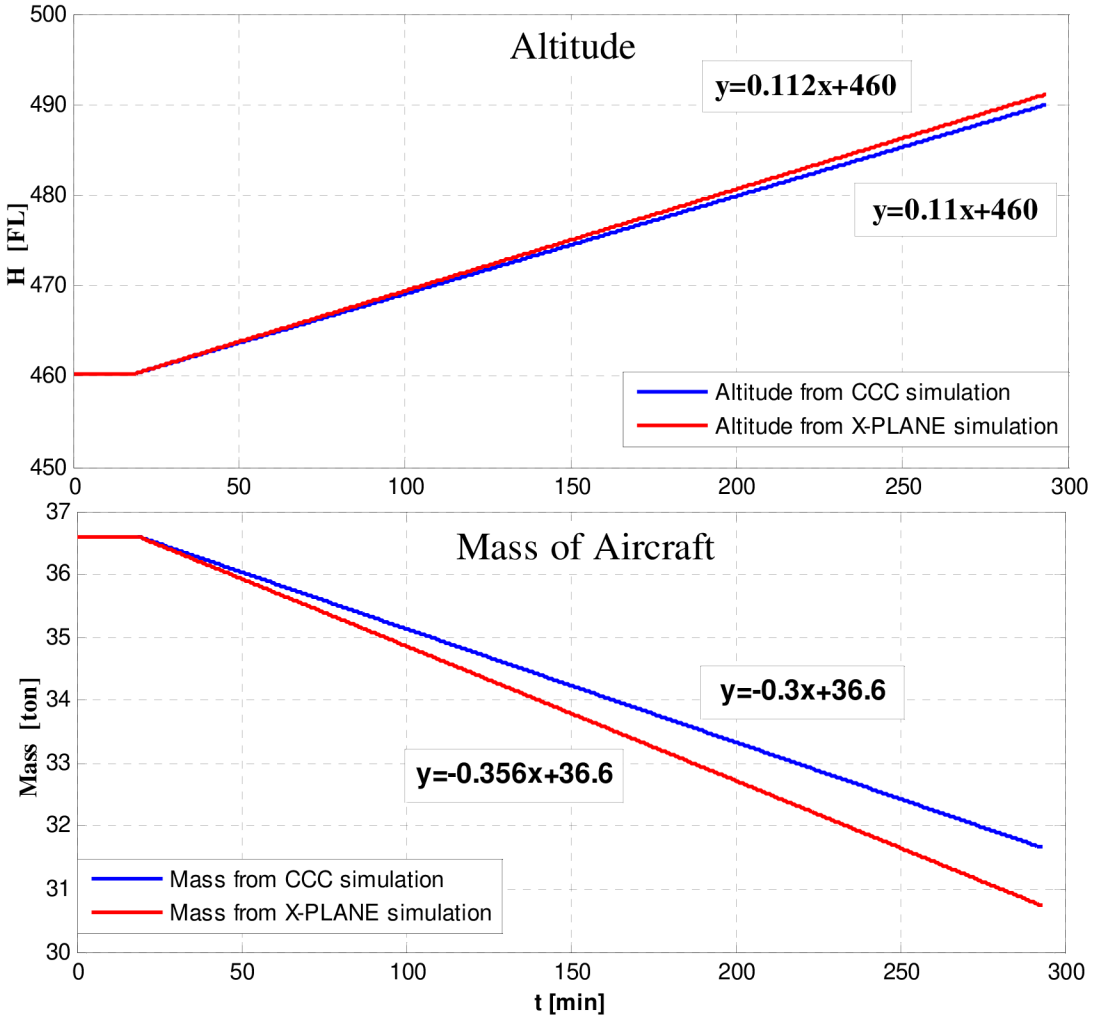

Figure 8.10: The CCC simulation vs. the X-plane CCC simulation

The initial and final mass of aircraft is defined by the measuring mass during simulation. The fuel consumption per distance flown is achieved by the difference between these mass.

In the Table 8.6, the main results of CCC simulation are summarized.

Parameter	Description
$\Delta m = 4907.88 kg$	Fuel consumption per distance flown
$\Delta m = 5863.39 kg$	Fuel consumption per distance flown (X-plane)
$RC = 11 ft / \min$	Vertical rate
$RC = 11.2 ft / \min$	Vertical rate (X-plane)
$L / D_{\max} = 19$	Maximum of L/D ratio
$L / D_{\max} = 19.2$	Maximum of L/D ratio (Piano)

Table 8.6: The main results of the CCC simulation

9. SIMULATION OF FUEL OPTIMAL CONTINUOUS CLIMBING CRUISE

In this chapter have been described results of the simulation fuel optimal Continuous Climbing Cruise (fuel optimal CCC). Firstly, the fundamental knowledge about the MATLAB Optimization Toolbox is written. There is shown, how the fuel optimal CCC can be obtained. Next, the results of simulation (e.g. altitude and airspeed characteristics) are shown in the section 9.2. In the last part of this chapter, an analysis of results is discussed.

9.1 OVERVIEW

The last task is determined the fuel optimal Continuous Climbing Cruise. The fuel optimal CCC is considered with respect of fuel consumption to distance flown. The fuel optimal CCC is defined by the optimal vertical rate respectively optimal setting of pitch angle. From chapter 8, the maximum value of L/D ratio is obtained if the pitch angle is equal to 3.2 degree for specific altitude = 460FL, weight = 36600kg and speed = 227.21ms^{-1}. The effective use of aerodynamic lift is in this case. This can be solution of optimization but the task is determined the optimal vertical rate with respect a fuel consumption per distance flown.

The optimal vertical rate can be achieved by analytic solutions. It is a calculation of the optimal trajectory with defined vertical rate. The definition of optimal trajectory is very complicated by analytical solutions. The analytical solution is not contained in the scope of thesis.

Furthermore, there was assumed the quadratic optimal control with LQ (Linear Quadratic) controller. For design the LQ controller, the linear model of controlled system is used and the optimal criterion is used in the quadratic form. The features of LQ controller are defined by the choice of constants and the optimization criterion. Because the linear aircraft model is not defined (see reasons in chapter 7) the LQ controller can't be proposed. There are two possibilities optimal control. The first one is the quadratic optimal regulation and the second one is the quadratic optimal tracking a reference signal. For calculate the optimal trajectory, the LQ controller cannot be used.

Finally, there is used to a mathematical optimization in the MATLAB optimization toolbox. The state space is searched by the one of the methods of numerical optimization. These methods are collectively included in the Toolbox OPTIM. The principle of these methods; the criterion function is minimized by the selected optimization method.

The theoretical background about the optimization toolbox is discussed. This background help reader understand how the fuel optimal CCC is obtained. In the chapter 9.1.2, the principle of optimization method is described in details.

9.1.1 Matlab Optimization Toolbox

In this section, the basic knowledge about mathematical optimization is discussed. The setting of optimization toolbox is used for simulation fuel optimal CCC.

Optimization Toolbox (OPTIM) is a graphical user interface for selecting a toolbox function, specifying optimization options, and running optimizations. The OPTIM provides the minimization functions, solution of linear and nonlinear equations, linear and nonlinear curve fitting, and etc. The minimization function is used for optimization Continuous Climbing Cruise. [16]

There is the function, which have been used for optimization: [16]

- Constrained nonlinear minimization (fmincon)

The graphical interface of Optimization Toolbox is shown in the appendix C. The five parameters have to be set for correctly simulation (see appendix C). Set up the Optimization Tool:

- Selected solver
- Specify function to minimize
- Start point
- Bounds
- Specify options

As a solver was usually used the fmincon method. Specify function to minimize is fminmass (see below). The success of optimization is dependent on the setting start point. If the start point set incorrect, the local minimum can be achieved. The limiting interval of iteration is defined by bounds, which have to be defined for solver fmincon. The some user tools (plot results) or parameters for better accuracy are set specify options.

9.1.2 Principle of Optimization Method

This section explains how to obtain a fuel optimal CCC and how the optimization toolbox is used for simulation. Both problems are closely related.

The distance flown is divided upon ten identical segments. In this segment, the setting of pitch angle can be different. The optimal pitch angle in each segment is found by optimization method. The optimal trajectory is defined by the vector of optimal pitch angles. There is shown the vector of optimal pitch angles.

$$Dtheta = [\theta_1\ \theta_2\ \theta_3\ \theta_4\ \theta_5\ \theta_6\ \theta_7\ \theta_8\ \theta_9\ \theta_{10}] \qquad (9.1)$$

This vector is input into the matlab function *selection(distance)*, where the vector is divided upon segments (see appendix B).

There is defined the criterion function *fminmass(v_Dtheta)*, which is input into the optimization toolbox (see appendix C). The criterion function is minimized by the selected optimization method (fmincon). In this function, The CCC simulation is running until the distance flown is equal to 4000 km. During the simulation the mass of

aircraft is measured. From initial and final mass of aircraft, the difference of mass is defined (*dm*). This difference of mass is output of the function *fminmass*.

9.2 RESULTS OF SIMULATION

There are presented the results of fuel optimal CCC simulation. The parameters of the simulation (e.g. initial vector $\mathbf{x}_0$, distance flown) are set same as in the chapter 8.

The fuel optimal CCC simulation is achieved by the vector of optimal pitch angles, [°]:

$$Dtheta_{optimal} = [3.1929\ 3.2048\ 3.1891\ 3.2052\ 3.1954\ 3.2055\ 3.2055\ 3.2040\ 3.1969\ 3.1999]$$

The Figure 9.1 shows block-diagram in MATLAB/SIMULINK, which is used for the fuel optimal CCC simulation. The SIMULINK schema is modified compare to block-diagram for the CCC simulation (see Figure 8.7). There is the block of MATLAB Function, which calls the function *selection*. The each segment of the vector $Dtheta_{optimal}$ is selected by this function.

The Figure 9.2 shows the graphical function of the important state variables for the fuel optimal CCC simulation. The true airspeed is controlled upon the constant desired value. But the pitch angle is controlled upon the desired value of $Dtheta_{optimal}$. Other assumptions are also validated as well as in the CCC simulation.

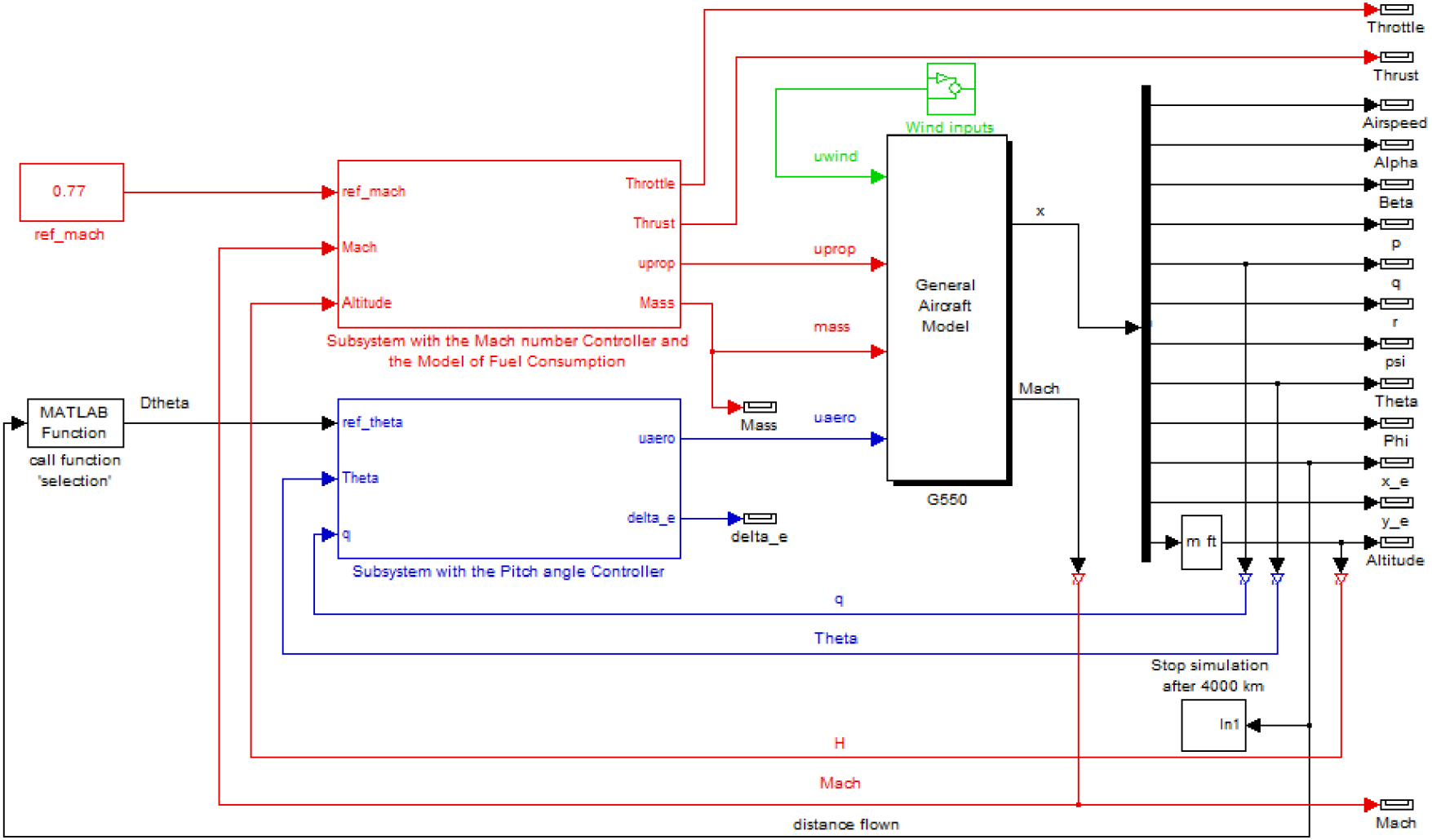

Figure 9.1: Block diagram for the fuel optimal CCC simulation

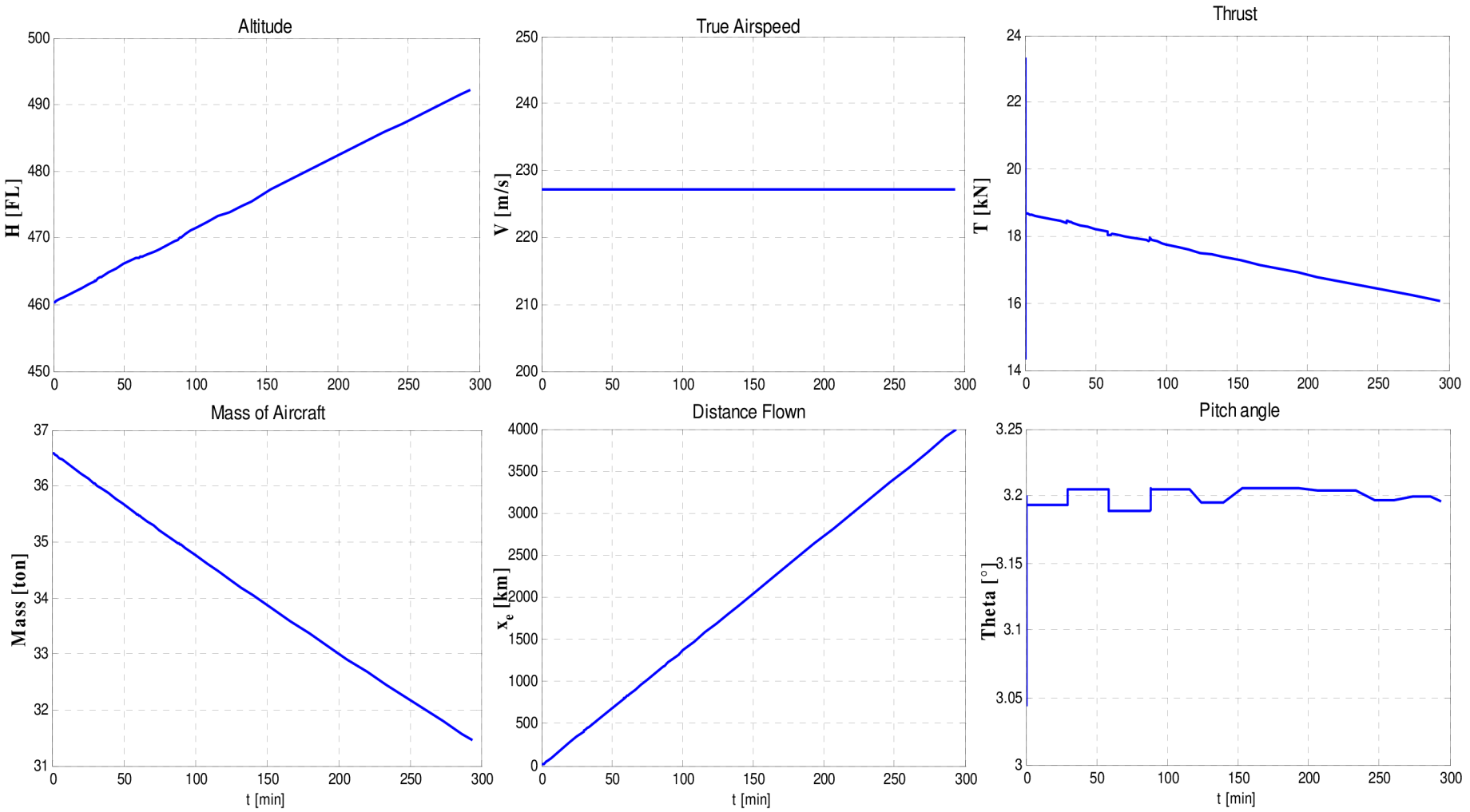

Figure 9.2: Graphical function of the state variables

9.3 DISCUSSION OF RESULTS

In this chapter, the main results of the fuel optimal CCC simulation are summarized. There are listed the setting of the Optimization Toolbox for the vector of optimal pitch angles. In next part, the fuel consumption per distance flown, and vertical rate are written for the fuel optimal CCC simulation.

The constrained criterion function is considered for searching the vector of optimal pitch angles. There is assumption that the reference pitch angle for aircraft model is limited, as in a real aircraft (see Table 8.1). Therefore, the constrained nonlinear minimization (fmincon) is used.

The result of optimization is depended on the setting of optimization toolbox parameters, especially the start point is very important.

The Table 9.2 shows the results of optimization process searching the vector of optimal pitch angles. At searching the vector of optimal pitch angles, the Optimization Toolbox has been set step by step according to Table 9.2. From Table 9.2, the mass difference is gradually decreased by the different starting point, reducing the bounds, and better setting of optimization toolbox (see the 7^{th} row). There has been used the better setting of Function tolerance, which specifies the termination tolerance for the objective function value.

From the results, the values of optimal vector are around the 3.2 degree. For this case, the maximum value of L/D ratio is achieved (see section 8.3).

In the Table 9.1, the main results of the fuel optimal CCC simulation are summarized. There is the comparison of fuel consumption per distance flown between the CCC simulation and the fuel optimal CCC simulation.

Parameter	Description
$RC = 11 ft / \min$	Vertical rate
$L / D = 19.2$	Maximum of L/D ratio
$\Delta m = 5135.38 kg$	The CCC Simulation
$\Delta m = 5133.67 kg$	The Fuel Optimal CCC Simulation

Table 9.1: The main results of the fuel optimal CCC simulation

Solver	Setting	Results
fmincon Specify options: default	Start point: $Dtheta_0 = [1.....1]$ Bounds: $\langle 1\,;\,5 \rangle$	Mass difference: $\Delta m = 5236.21kg$
fmincon Specify options: default	Start point: $Dtheta_0 = [5.....5]$ Bounds: $\langle 1\,;\,5 \rangle$	Mass difference: $\Delta m = 5177.12kg$
fmincon Specify options: default	Start point: $Dtheta_0 = [3.....3]$ Bounds: $\langle 1\,;\,5 \rangle$	Mass difference: $\Delta m = 5149.56kg$
fmincon Specify options: default	Start point: $Dtheta_0 = [3.2.....3.2]$ Bounds: $\langle 2\,;\,4 \rangle$	Mass difference: $\Delta m = 5135.12kg$
fmincon Specify options: default	Start point: $Dtheta_0 = [3.2.....3.2]$ Bounds: $\langle 2.5\,;\,3.5 \rangle$	Mass difference: $\Delta m = 5134.56kg$
fmincon Specify options: default	Start point: $Dtheta_0 = [3.2.....3.2]$ Bounds: $\langle 3\,;\,3.3 \rangle$	Mass difference: $\Delta m = 5133.92kg$
fmincon Specify options: Function tolerance = $\mathbf{1e^{-8}}$	Start point: $\mathbf{Dtheta_0 = [3.2.....3.2]}$ Bounds: $\mathbf{\langle 3\,;\,3.3 \rangle}$	Mass difference: $\mathbf{\Delta m = 5133.67kg}$

Table 9.2: The optimization process of searching the fuel optimal vector (Dtheta)

.

10. CONCLUSION

This master‘s thesis focused on modeling the Continuous Climbing Cruise type of flight and determining the fuel optimal vertical flight profile in the cruise phase. Firstly, the aircraft equations of motion were described in detail, including equations of inertial reference position of the aircraft in the coordinate system and equations of forces and moments actuating upon the aircraft.

Then the numerical nonlinear aircraft model was compiled based on the referenced equations of motion and the theoretical background of aerodynamics, propulsive, gravity, and wind forces and moments. Although this nonlinear aircraft model allows to be applied to any type of aircraft, for the purpose of this work the model has been applied to the Gulfstream G550 jet plane. Further, the aircraft model has been extended to take into account modeling the fuel consumption. This resulted in more realistic the flight simulation, because the aircraft mass is gradually decreasing in connection to the fuel consumption.

The simulation of Continuous Climbing Cruise based on the aircraft model was then validated with the aid of the Continuous Climbing Cruise of the X-plane flight simulator. Two controllers for the Continuous Climbing Cruise simulation were proposed. The Pitch Angle Controller is used to control the pitch angle of the aircraft model, affecting the rate of climb. The Mach number Controller is used to control the airspeed of the aircraft model. Both simulations have been compared, resulting in the conclusion of the CCC simulation matching the X-Plane flight simulator CCC simulation. A slight difference found is caused by different fuel consumption. The higher rate of climb of the X-Plane CCC simulation is due to this difference.

Finally, the fuel optimal Continuous Climbing Cruise has been researched with the objective of optimization of the vertical flight profile. A mathematical optimization technique in the MATLAB optimization toolbox has been employed for this task. The principle of this method is as follows - the optimal setting of the vector of pitch angles is determined with respect to the fuel consumption per distance flown. The fuel consumption in the fuel optimal CCC simulation came out lower than the fuel consumption in the CCC simulation, but the difference can be considered neglect able.

The result of this thesis shows us that the fuel optimal vertical profile can be achieved by the Continuous Climbing Cruise mode of flight while keeping the maximum Lift to Drag ratio.

The analytical solution of determination the fuel optimal trajectory could be the aim of the future work.

11. REFERENCES

[1] RAUW, M.O.: *FDC 1.4 - A Simulink Toolbox for Flight Dynamics and Control Analysis.* Zeist, The Netherlands, 1997 (draft version 7: Haarlem, The Netherlands, 2001), ISBN: 90-807177-1-1.

[2] DUKE, E.L.; PATTERSON, B.P.; ANTONIEWICZ, R.F.; KRAMBEER, K.D.: *Derivation and Definition of a Linear Aircraft Model.* NASA RP - 1207, 1988.

[3] ROSKAM, J.: *Airplane Flight Dynamics and Automatic Flight Controls*. Design, Analysis and Research Corporation, Lawrence, Kansas, 2001, ISBN 1-884885-17-9.

[4] LAN CH-T.E., ROSKAM J.: *Airplane Aerodynamics and Performance*. Design, Analysis and Research Corporation, Lawrence, Kansas, 1997. ISBN 1-884885-44-6.

[5] ANONYMOUS. *New FM Pilot's Guide* [online]. c2005, Smiths Thales, [cit. 2011-05-20]. Available at: <http://www.smartcockpit.com/pdf/plane/airbus/A320/misc/0004/>

[6] BENSON, T. *Four Forces on an Airplane* [online]. c2008, NASA, last revision 2010-09-09 [cit. 2011-05-20]. Available at: <http://www.grc.nasa.gov/WWW/K-12/airplane/forces.html\>

[7] BENSON, T. *The Drag Coefficient* [online]. c2008, NASA, last revision 2010-08-10 [cit. 2011-05-20]. Available at: <http://www.grc.nasa.gov/WWW/K-12/airplane/dragco.html>

[8] JACKSON M.: *Sensitivity of Trajectory Prediction in Air Traffic Management and Flight Management Systems*. The University of Minnesota, 1997. 175s. Dissertation thesis. Yiyuan Zhao, Advisor.

[9] BAKSHT, D.; CHANG, A.; STONE, M.; THOMPSON, R.: *Modeling and Performance Analysis of Long-Range Business Jet Aircraft and Turbofan Power Plants* [online]. c2002, Department of Mechanical Engineering, University of Texas at Austin, [cit. 2011-05-20]. Available at: <http://www.silverflame.com/~aven0314/Portfolio/turbofan.pdf>

[10] ANONYMOUS. *Commons.wikimedia* [online]. c2005, last revision 2009-08-16 [cit. 2011-05-20]. Available at: <http://commons.wikimedia.org/wiki/File:Turbofan_operation_%28lbp%29.png>

[11] ANONYMOUS. *Gulfstream* [online]. c2011, Gulfstream Aerospace Corporation, [cit. 2011-05-20]. Available at: < http://www.gulfstream.com/products/g550/>

[12] ANONYMOUS. *G550-Aircraft General* [online]. c2005, Gulfstream Aerospace Corporation, last revision 2007-03-27 [cit. 2011-05-20]. Available at:<http://www.smartcockpit.com/pdf/plane/gulfstream/G550/systems/0027/>

[13] ANONYMOUS. *G550-Flight Controls* [online]. c2005, Gulfstream Aerospace Corporation, last revision 2007-03-27 [cit. 2011-05-20]. Available at:<http://www.smartcockpit.com/pdf/plane/gulfstream/G550/systems/0040/>

[14] ANONYMOUS. *Piano-X*[online]. c2010, [cit. 2011-05-20]. Available at: <http://www.lissys.demon.co.uk/>

[15] ANONYMOUS. *Turbofan Engine System* [online]. c1984-2011, The MathWorks, Inc., [cit. 2011-05-20]. Available at :< http://www.mathworks.com/help/toolbox/aeroblks/turbofanenginesystem.html>

[16] COLEMAN, T.; BRANCH, M.A.; GRANCE, A.: *Optimization Toolbox User's Guide*. The MathWorks, Inc., 2003, version 2.3

[17] ANONYMOUS. *Lift and Drag Curves* [online]. c1995-2011, ALLSTAR Network, [cit. 2011-05-20]. Available at: <http://www.allstar.fiu.edu/aero/lift_drag.htm>

[18] PIVOŇKA, P.: *Optimalizace regulátorů*. Skriptum VUT Brno, 2005, 112s

[19] STEVENS, B., L., LEWIS, F., L.: *Aircraft Control and Simulation*. John Wiley and Sons, Inc., N.Y. 1992, ISBN 0-471-61397-5. 2nd edition ISBN: 0-471-37145-9, 2004

[20] BENSON, T. *The Lift Coefficient* [online]. c2008, NASA, last revision 2009-04-09 [cit. 2011-05-20]. Available at: <http://www.grc.nasa.gov/WWW/K-12/airplane/liftco.html>

[21] BENSON, T. *Lift to Drag ratio* [online]. c2008, NASA, last revision 2010-08-28 [cit. 2011-05-20]. Available at: <http://www.grc.nasa.gov/WWW/K-12/airplane/ldrat.html>

[22] ANONYMOUS. *Aircraft Performance 2 Summary* [online]. Aerospace Students, [cit. 2011-05-20]. Available at: <http://www.aerostudents.com/secondyear/aircraftPerformance2.php>

[23] ANONYMOUS. *Parasitic Drag* [online]. last revision 2011-03-14 [cit. 2011-05-20]. Available at: < http://en.wikipedia.org/wiki/Form_drag#Form_drag>

[24] ANONYMOUS. *Gulfstream G550 (GV-SP) sample analysis*[online]. last revision Feb. 2006 [cit. 2011-05-20]. Available at: < http://www.lissys.demon.co.uk/samp2/index.html>

ENCLOSURE LIST

Appendix A Reference Frames
Appendix B Program Code
Appendix C GUI of MATLAB Optimization Toolbox

APPENDIX A

REFERENCE FRAMES

Definitions [1] [2]

Body-fixed reference frame F_B: This is a right-handed orthogonal reference system which has its origin O_B in the center of gravity of the aircraft. The $X_BO_BZ_B$ plane coincides with the aircraft's plane of symmetry if it is symmetrical, or it is located in a plane, approximating what would be the plane of symmetry. The X_B-axis is directed toward the nose of the aircraft, the Y_B-axis points to the right wing ('starboard'), and the Z_B-axis points toward the bottom of the aircraft.

Flight-path or wind reference frame F_W: This reference frame, also called the wind reference frame, has its origin in the center of gravity of the aircraft. The X_W-axis is aligned with the velocity vector of the aircraft and the Z_W-axis coincides with the Z_S-axis.

Vehicle-carried vertical reference system F_V: has its origin at the center of gravity of the aircraft. The X_V-axis is directed to the North, the Y_V-axis to the East, and the Z_V-axis points downwards (along the local direction of gravity). These reference axes are always parallel to the Earth-fixed reference axes, although the origin O_V moves relatively to the Earth-fixed reference frame.

Earth-fixed reference frame F_E: This reference frame, also called the topodetic reference frame is a right-handed orthogonal system which is considered to be fixed in space. Its origin can be placed at an arbitrary position, but is chosen to coincide with the aircraft's center of gravity at the start of a flight test manoeuvre. The Z_E-axis points downwards, parallel to the local direction of gravity. The X_E-axis is directed to the North, the Y_E-axis to the East.

Relationships between the reference frames [1] [2]

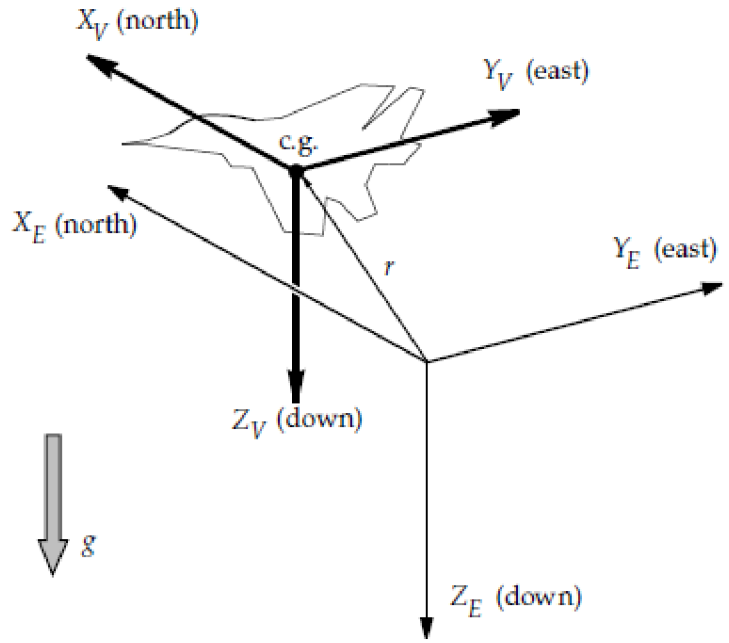

Figure A.1: Relationship between the Vehicle-carried vertical and the Earth-fixed reference frame [1]

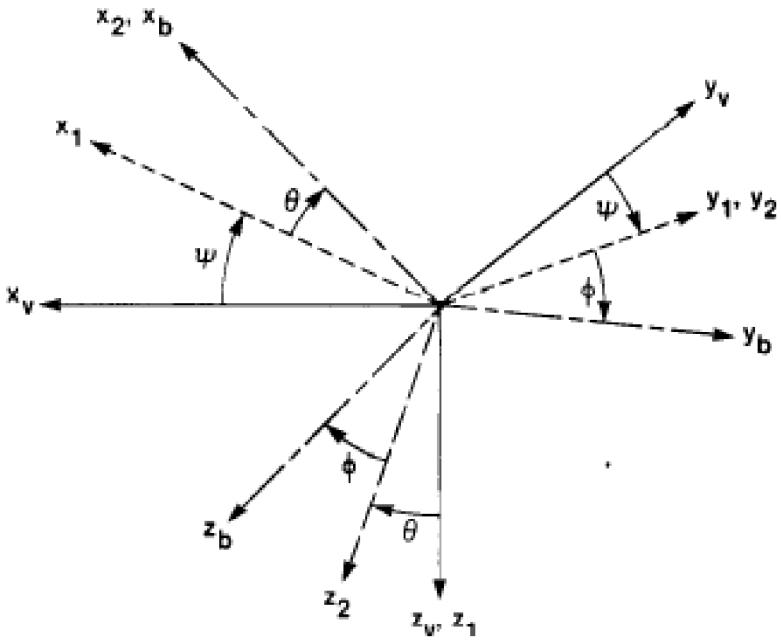

Figure A.2: Relationship between the Vehicle-carried vertical and the Body-fixed reference frame [2]

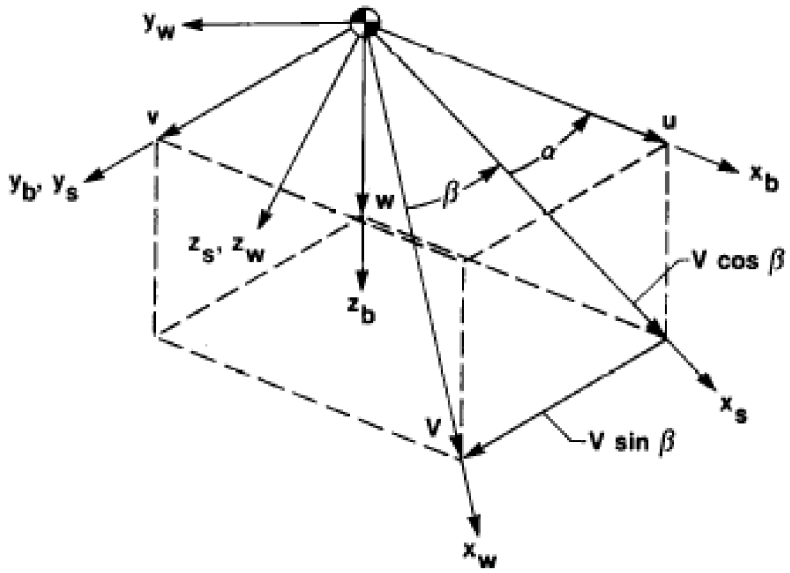

Figure A.3: Relationship between the Body-fixed and the Flight-path reference frame [2]

APPENDIX B

FUNCTION *"SELECTION"*

```
function THETA=selection(distance)

global Dtheta;

THETA = Dtheta(1)*pi/180;
    if distance>=400000 && distance<=800000
        THETA = Dtheta(2)*pi/180;
    elseif distance>=800000 && distance<=1200000
        THETA = Dtheta(3)*pi/180;
    elseif distance>=1200000 && distance<=1600000
       THETA = Dtheta(4)*pi/180;
    elseif distance>=1600000 && distance<=2000000
       THETA = Dtheta(5)*pi/180;
    elseif distance>=2000000 && distance<=2400000
       THETA = Dtheta(6)*pi/180;
    elseif distance>=2400000 && distance<=2800000
       THETA = Dtheta(7)*pi/180;
    elseif distance>=2800000 && distance<=3200000
       THETA = Dtheta(8)*pi/180;
    elseif distance>=3200000 && distance<=3600000
       THETA = Dtheta(9)*pi/180;
    elseif distance>=3600000 && distance<=4000000
       THETA = Dtheta(10)*pi/180;
    end
end
```

FUNCTION *"FMINMASS"*

```
function dm=fminmass(v_Dtheta)

global Dtheta

Dtheta=v_Dtheta;

sim('G550_fuel_optimal_CCC_simulation',[]);

dm=Mass.signals.values(1,1)-Mass.signals.values(end,1);
end
```

FUNCTION *"GETATMOSPHERE"*

```
function y_atm = GetAtmosphere(Alt)

Lapse=0.0065;      %K/m       - temperature lapse rate
hPause=11000;      %m         - bound altitude of tropopause
T0=288.15;         %K         - air temperature at sea level
T0Pause=T0-71.5;   %K         - air temperature in tropopause
p0=101325;         %Pa        - air pressure at sea level
p0Pause=22632;     %Pa        - pressure in tropopause
M=0.0289644;       %kg/mol    - molar mass of dry air
R=8.31447;         %J/(mol.K) - universal gas constant
g0=9.80665;        %m/s       - acceleration of gravity

if Alt<11000
      g=g0*(6371020/(6371020+Alt))^2;
      T=T0-Lapse*Alt;
      p=p0*(1-(Lapse*Alt)/T0)^(g*M/(R*Lapse));
      Ro=p*M/(R*T);
      mi=(1.458*10^(-6)*T^1.5)/(T+110.4);
else
      g=g0*(6371020/(6371020+Alt))^2;
      T=T0Pause;
      p=p0Pause*exp(-g*(Alt-hPause)/(R/M*T0Pause));
      Ro=p/(T*R/M);
      mi=(1.458*10^(-6)*T^1.5)/(T+110.4);
end
y_atm=[Ro; p; T; mi; g];
```

APPENDIX C

GUI OF MATLAB OPTIMIZATION TOOLBOX [16]